ELSEVIER

Contents lists available at ScienceDirect

# Journal of Cleaner Production

journal homepage: www.elsevier.com/locate/jclepro





# Multi-objective collaborative agreements amongst shipping lines and marine terminal operators for sustainable and environmental-friendly ship schedule design

## Maxim A. Dulebenets

Department of Civil & Environmental Engineering, Florida A&M University-Florida State University (FAMU-FSU) College of Engineering, 2525 Pottsdamer Street, Building A, Suite A124, Tallahassee, FL, 32310-6046, USA

#### ARTICLE INFO

Handling editor. M.T. Moreira

Keywords:
Maritime transportation
Liner shipping
Ship scheduling
Environmental sustainability
Multi-objective optimization
Collaborative agreements

#### ABSTRACT

Oceangoing ships transport a significant amount of different goods across the globe. The seaborne trade is expected to continue its growth despite the COVID-19 pandemic. The International Maritime Organization considers the amount of emissions produced by oceangoing ships as substantial. Shipping lines have to explore innovative and effective alternatives to meet challenging emission reduction targets. This study proposes a new type of collaborative agreements amongst shipping lines and marine terminal operators, where the shipping line is not only able to select the marine terminal for the ship service at every port of the shipping route but also request the appropriate arrival time window and handling rate. A multi-objective mathematical model is developed to capture the proposed collaborative agreements. The first objective of the model minimizes the cost components that are mostly driven by the economic perspectives, while the second one directly captures the environmental perspectives as well. A novel customized exact multi-objective optimization method, inspired by the ε-constraint method and the goal programming method, is developed to address the problem. The computational experiments are conducted for the Europe Pakistan India Consortium 2 (EPIC-2) shipping route. The results show that the developed solution method is able to generate the Pareto Fronts with sufficient solution density. The experiments also demonstrate that the proposed multi-objective mathematical model could facilitate the analysis of trade-offs amongst the economic and environmental perspectives in the ship schedule design. Furthermore, the importance of effective collaborative agreements amongst shipping lines and marine terminal operators is showcased as well.

# 1. Background

A significant amount of goods are transported by oceangoing ships around the world. More specifically, the global seaborne trade reached 11.08 billion tons in 2019 with more than 800 million twenty-foot equivalent units (a.k.a., "TEUs") handled at ports worldwide (UNCTAD, 2020). The COVID-19 pandemic had significant effects on liner shipping and maritime transportation overall. Some marine container terminals decided to close due to the fact that the terminal employees were infected with the virus (JOC, 2020). Certain ships were required to wait for an extended period of time before they could be served due to container terminal shutdowns. Temporary terminal congestion and shutdowns resulted in substantial supply chain disruptions. Although the seaborne trade volumes reduced approximately by 4% during the year of 2020 due to the COVID-19 disruptions, the

seaborne trade is expected to recover and expand again in the year of 2021 (UNCTAD, 2020). Sustainable container shipping is essential for the future development of maritime transportation. Shipping lines have to keep in mind not only the economic perspectives that are associated with serving the existing and new customers along with attaining the target profit margins but also the environmental perspectives as well. The amount of emissions produced by oceangoing ships is still ranked as "high" by the International Maritime Organization (IMO) and other relevant agencies (UNCTAD, 2020).

Different measures have been introduced to decrease the amount of greenhouse gas emissions (mostly  $CO_2$ ,  $CH_4$ , and  $N_2O$ ) and nongreenhouse gas emissions (mostly  $NO_x$ ,  $SO_x$ , and PM) from maritime transportation. In order to reduce the amount non-greenhouse gas emissions, the IMO established a number of Emission Control Areas (ECAs) in particular geographical regions, including the English

E-mail address: mdulebenets@eng.famu.fsu.edu.

Channel, the Baltic Sea, the North Sea, and the Northern American coastline (Yang et al., 2019; Dong and Lee, 2020; Ma et al., 2021). Furthermore, the Chinese authorities declared certain areas of the Chinese coastline as ECAs (i.e., the Pearl Delta, the Yangtze Delta, and the Bohai Bay). The ships sailing inside ECAs are mandated to use the fuel with no more than 0.10% m/m (mass by mass) of sulfur. Starting January 01, 2020, a new limit on the content of sulfur was introduced by the IMO for ships sailing outside the designated ECAs (the regulation known as "IMO, 2020"). Based on this new regulation, the ships that are even sailing outside ECAs are now required to use the fuel with the sulfur limit of 0.50% m/m, which is a substantial change when comparing to the previous limit of 3.5% m/m (IMO, 2021a). Before the IMO 2020 regulation, many ships were using heavy fuel oil with  $\approx 3.5\%$  of sulfur when sailing outside ECAs. With the new regulation, the vast majority of ships must use very low sulfur fuel oil (VLSFO) to meet the fuel sulfur content limit. The reduction in sulfur emissions is expected to provide major health and environmental benefits, especially in the vicinity of coastal areas.

Some ECAs (e.g., Northern American ECAs) impose restrictions not only on SO<sub>x</sub> bust also on NO<sub>x</sub> and PM as well. While PM emissions are sulfur-based and can be controlled by the sulfur content in fuel, NO<sub>v</sub> emissions are controlled by setting the specific requirements on ship engines based on their maximum sailing speed (Dulebenets, 2016). As for greenhouse gas emissions, the IMO introduced a new regulation on energy efficiency for ships in 2011, which was the first attempt to regulate the amount of greenhouse gas emissions by attaining a specific "Energy Efficiency Design Index" for ships (IMO, 2021b). The "Energy Efficiency Design Index" is computed based on the fuel type used as well as the ship technical specifications. The ship sailing speed reduction strategy (a.k.a., "slow steaming") has been widely used as well, as it allows shipping lines substantially reducing greenhouse and non-greenhouse gas emissions (Dong and Lee, 2020). Some ports even provide monetary incentives to shipping lines for sailing speed reduction when ships are approaching the associated coastal areas (Zhuge et al., 2021). Shipping lines continue exploring other strategies for reducing the emissions produced that include, but are not solely limited to, the following (Bouman et al., 2017; Peng et al., 2021; Tang et al., 2021): (i) use of shore power when ships are anchored at berthing positions instead of using auxiliary engines and burning additional fuel throughout the service of ships at ports; (ii) application of various carbon taxation schemes; (iii) improvement of ship design (e.g., use a specific shape of the ship hull); (iv) enhancing the operation of power and propulsion systems; (v) consideration of alternative fuel and energy sources (e.g., biofuels, liquefied natural gas, solar energy); (vi) improvement of ship maintenance activities; and others.

Nevertheless, many of the aforementioned alternatives may not be effective enough to meet the long-term IMO target of reducing the total annual greenhouse gas emissions by 50% when comparing the 2008 and 2050 emission levels (UNCTAD, 2020). In order to achieve the IMO targets, shipping lines have to explore other innovative alternatives. Collaborative agreements amongst shipping lines and other industry partners (e.g., marine terminal operators that are directly involved in service of the arriving ships at ports) can be an effective option. Unlike many existing alternatives for emission reduction, collaborative agreements do not require significant monetary investments and can be executed amongst the relevant stakeholders by simply utilizing the available resources in a more effective manner. However, the collaborative agreements that have been proposed and evaluated in the ship scheduling literature are quite limited. In particular, most of the existing ship scheduling studies on collaborative agreements assume that multiple arrival time windows and/or handling rates can be offered by the terminal operator to the shipping line at every port (or certain ports) of the shipping route (Dulebenets et al., 2021).

The flexibility in terms of arrival time window and/or handling rate selection allows shipping lines making necessary adjustments in ship schedules and improving the overall ship schedule efficiency (e.g., select a later time window at the next port and use a lower speed when sailing to that port in order to decrease the fuel consumption and associated emissions). In reality, more comprehensive collaborative agreements may exist at ports, where terminal operators may collaborate with each other and share the available capacity to serve the arriving ships (Imai et al., 2008) – see Fig. 1, where terminal operators "MT-1", "MT-2", and "MT-3" have a collaborative agreement and share the available capacity (i.e., berthing space, arrival time windows, handling equipment, etc.) for the ship service. Such collaborative agreements may provide more resources and flexibility for serving the arriving ships.

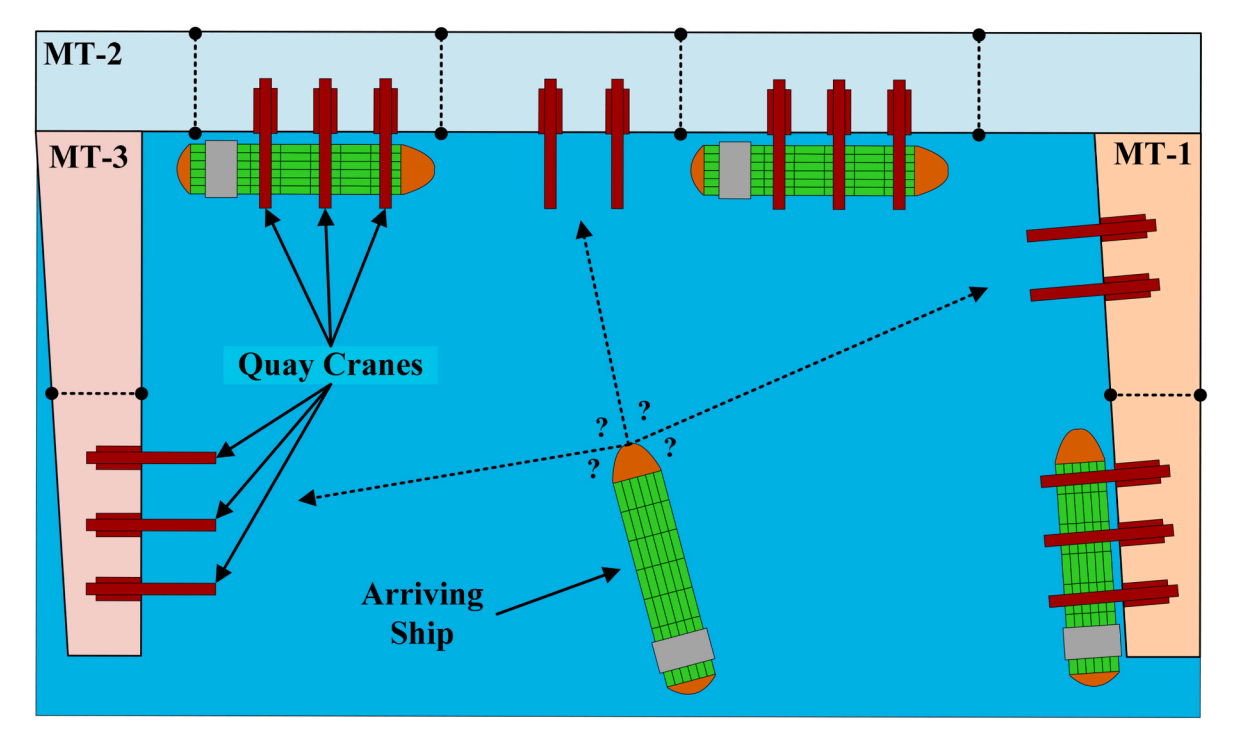


Fig. 1. Collaborative service of the arriving ships at a port.

Considering the increasing attention of the communities to the global environmental problems and the need for the alternative ways of decreasing the emissions produced by oceangoing ships, this study proposes a novel multi-objective mathematical model that explicitly captures comprehensive collaborative agreements amongst shipping lines and marine terminal operators, based on which the shipping line is not only able to select the marine terminal for the ship service at every port of the shipping route but also request the appropriate arrival time window and handling rate. The first objective of the model minimizes the cost components that are mostly driven by the economic perspectives, while the second one directly captures the environmental perspectives as well. A novel customized exact multi-objective optimization method, inspired by the  $\varepsilon$ -constraint method and the goal programming method, is developed to solve the problem. The effectiveness of the presented multi-objective model and the proposed solution method are demonstrated for a real-life shipping route. The remaining sections of the manuscript focus on the following aspects. The second section provides a concise overview of the previous studies that are relevant to the theme of this research. The decision problem studied herein and its multi-objective mathematical formulation are formally introduced in the third and fourth sections, respectively. The fifth section presents the developed exact multi-objective optimization method, whereas the sixth section describes the computational experiments along with managerial insights revealed. The key conclusions are provided in the last section.

## 2. Literature review

#### 2.1. Review of the relevant studies

A substantial number of studies on ship scheduling in liner shipping have been conducted over the past years (Meng et al., 2014; Song et al., 2015; Gürel and Shadmand, 2019; Wang et al., 2019; Qi et al., 2021; Wang and Wang, 2021). However, most of these numerous studies do not explicitly model collaborative agreements amongst shipping lines and marine terminal operators at ports (Dulebenets et al., 2021). More specifically, most of the studies simply assume that each ship should arrive within a previously negotiated arrival time window at every port, and the duration of ship handling time at every port is fixed. In reality, many terminal operators are typically able to provide more than just one arrival time window and more than just one handling rate for service of the arriving ships. The study conducted by Fagerholt (2001) was one of the first efforts that attempted to model more realistic operational features of the ship service at ports by introducing a "soft time window" concept, based on which the ships could arrive at every port outside of the previously negotiated arrival time window. However, additional costs (i.e., "inconvenience costs") were applied for the shipping line in case of ship arrivals outside the agreed time windows. Wang et al. (2014) and Alharbi et al. (2015) proposed the mathematical models that captured the availability of multiple arrival time windows for service of ships at every port of a given shipping route. However, ship handling times at ports were assumed to be fixed. Wang et al. (2015) investigated various collaborative mechanisms amongst shipping lines and terminal operators, based on which every shipping line had to provide a certain utility value to the terminal operator at every port depending on the actual ship arrival time.

Liu et al. (2016) presented an alternative type of collaborative agreements amongst shipping lines and marine terminal operators, based on which the shipping line could request handling rates that have higher productivities to reduce the ship handling time at ports. The port time savings could be further used at sea to select lower speed of ships when sailing to subsequent ports of the shipping route and decrease the ship fuel consumption. However, the study did not model potential availability of multiple arrival time windows at ports. Some of the recent studies on ship scheduling addressed the latter drawback and proposed new types of collaborative agreements, which not only captured the availability of multiple arrival time windows at ports but also the

availability of multiple handling rates during each time window (Dulebenets, 2018; Pasha et al., 2020). A more comprehensive collaborative mechanism was developed by Dulebenets (2019), where the marine terminal operator could offer multiple arrival time windows, start and end times for the available time windows, as well as multiple handling rates for service of the arriving ships. A set of comprehensive experiments were performed to compute potential monetary benefits that could be attained by shipping lines from the proposed form of collaborative agreements.

All the aforementioned studies modeled collaborative agreements amongst shipping lines and marine terminal operators primarily focusing on the ship scheduling decisions (e.g., port arrival/departure times, ship sailing speed at voyage legs, number of ships required for deployment) without explicitly considering the berth scheduling decisions. Another group of relevant studies specifically captures collaborative agreements solely amongst terminal operators at a given port and models the berth scheduling decisions (e.g., assignment of ships to terminals, assignment of ships to berthing positions, ship service order at each berthing position). Imai et al. (2008) is considered as a pioneering study on berth scheduling with collaborative agreements amongst terminal operators, where the ships with excessive waiting times could be shifted from a multi-user terminal and be served at the external terminal. The objective of the presented berth scheduling model minimized the total ship service time at the external terminal. Subsequently, Peng et al. (2015) studied a collaborative berth scheduling problem, where it was assumed that the operators of adjacent marine terminals could share the berthing space and the yard space for service of ships. Dulebenets et al. (2018) developed a Memetic Algorithm for a berth scheduling problem, assuming that some of the arriving ships could be shifted from a multi-user terminal and be served at the external terminal during particular time windows. The computational experiments demonstrated the effectiveness of the proposed solution method and potential benefits of the presented collaborative berth scheduling policy.

More recently, Torkian et al. (2020) proposed a collaborative berth scheduling policy for the Shahid Rajaee Port (Iran), where two adjacent terminals of the port could share the available resources for service of the arriving ships. An exact optimization method (CPLEX) was further deployed to solve the developed mathematical formulation. The results from the conducted numerical experiments demonstrated the effectiveness of the proposed collaborative berth scheduling policy and a significant waiting time reduction for the arriving ships, especially during high demand periods. Cho et al. (2021) studied an integrated decision problem of berth allocation and quay crane assignment, assuming that the arriving ships could be re-assigned for service amongst different multi-user terminals of the same port. A set of heuristic methods based on the Filtered Beam Search and Greedy Randomized Adaptive Search Procedure were used to address the problem. A set of experiments were then performed for the Port of Busan (Korea). It was concluded that the proposed methodology would be advantageous for marine terminal operators, considering the growing volumes of international seaborne trade in the Asia-Pacific region. For a more detailed review of the general ship scheduling studies, the interested readers can refer to extensive survey studies conducted by Meng et al. (2014) and Dulebenets et al. (2021). Moreover, a detailed description of the general berth scheduling studies can be found in Bierwirth and Meisel (2015) and Carlo et al. (2015).

## 2.2. Literature summary and contributions of this work

A concise summary of the reviewed studies that are the most relevant to the present work is presented in Table 1 that contains the following information for each study: author(s) of the study, year of publication, theme of the study, objective of the optimization model proposed, solution methodology adopted, and main considerations that were captured by the study. After a critical review of the relevant studies on collaborative agreements in ship scheduling and berth scheduling, two

**Table 1**Review summary for the most relevant studies.

a/ a	Author(s)	Year	Theme	Model Objective	Solution Methodology	Main Considerations
1	Fagerholt	2001	VSP	Minimize the total cost of route service	Heuristic	Application of the "soft time window" concept
2	Imai et al.	2008	BSP	Minimize the total service time of ships	EA	Ships with excessive waiting times could be shifted to another terminal
3	Wang et al.	2014	VSP	Minimize the total cost of route service	Iterative optimization method	Multiple arrival time windows for service of ships
4	Alharbi et al.	2015	VSP	Minimize the total cost of route service	Iterative optimization method	Multiple arrival time windows for service of ships
5	Peng et al.	2015	BSP	Minimize the total service time of ships + yard space equilibrium	EA	Operators of adjacent marine terminals could share the berthing space and the yard space for service of ships
6	Wang et al.	2015	VSP	Maximize the total utility of shipping lines	Heuristic	Consideration of the utility value based on the actual ship arrival time
7	Liu et al.	2016	VSP	Minimize the total cost of route service	Iterative optimization method	Multiple handling rates for service of ships
8	Dulebenets	2018	VSP	Minimize the total cost of route service	Iterative optimization method	Multiple arrival time windows and handling rates for service of ships
9	Dulebenets et al.	2018	BSP	Minimize the total cost of ship service	MA	Some of the arriving ships could be shifted to another terminal during particular time windows
10	Dulebenets	2019	VSP	Minimize the total cost of route service	CPLEX	Consideration of start and end times for arrival time windows
11	Pasha et al.	2020	VSP	Maximize the total profit from route service	BARON	Multiple arrival time windows and handling rates for service of ships
12	Torkian et al.	2020	BSP	Minimize the total cost of ship service	CPLEX	Two adjacent terminals of the port could share the available resources for service of the arriving ships
13	Cho et al.	2021	BSP	Minimize the total cost of ship service	FBS; GRASP; Heuristic	The arriving ships could be re-assigned for service amongst different multi-user terminals of the same port

Abbreviations Used: Theme [VSP – vessel scheduling problem; BSP – berth scheduling problem]; Solution Methodology [BARON – optimization solver; CPLEX – optimization solver; EA – Evolutionary Algorithm; FBS – Filtered Beam Search; GRASP – Greedy Randomized Adaptive Search Procedure; MA – Memetic Algorithm].

major groups of studies were identified. The first group of studies focuses on collaborative agreements amongst shipping lines and marine terminal operators, assuming that multiple arrival time windows and/or handling rates can be offered by the terminal operator to the shipping line at every port (or certain ports) of the shipping route. This group of studies primarily captures the ship scheduling decisions without explicitly considering the berth scheduling decisions and potential collaborative agreements that may exist amongst terminal operators. On the other hand, the second group of studies specifically captures collaborative agreements solely amongst terminal operators at a given port and models the berth scheduling decisions, assuming that certain ships can be diverted for service to the collaborating terminal. However, the preferences of a shipping line are not explicitly considered when modeling the diversion of ships. In fact, the shipping line may even change its original ship schedule if terminal operators of a given port have collaborative agreements in place and share the available resources (e.g., an alternative time window and/or handling rate can be selected at the collaborating terminal for the ship service to use a lower speed when sailing to the next port and decrease the fuel consumption as well as the associated emissions). Considering the aforementioned limitations in the state-of-the-art and increasing attention of the communities to the global environmental problems, this study offers the following main contributions:

- ✓ A novel mathematical model is proposed to explicitly capture comprehensive collaborative agreements amongst shipping lines and marine terminal operators, where the shipping line is not only able to select the marine terminal for the ship service at every port of the shipping route but also request the appropriate arrival time window and handling rate.
- ✓ The collaborative agreements are evaluated in multi-objective settings considering both economic and environmental perspectives. Emissions produced by ships at sea and by designated handling equipment throughout the ship service at ports are directly accounted for by the model.
- A novel customized exact multi-objective optimization method, inspired by the ε-constraint method and the goal programming method, is developed to solve the problem.

✓ A set of computational experiments are performed for a real-life shipping route to showcase the effectiveness of the presented multi-objective mathematical model and the proposed solution method.

# 3. Problem description

This section of the manuscript provides more information regarding the ship scheduling decision problem addressed in this study. The following aspects are further discussed in detail: (i) ship voyage; (ii) fuel consumption modeling; (iii) marine terminal operations and collaborative agreements; (iv) port service frequency requirements; (v) container inventory throughout the ship voyage; and (vi) emission modeling.

# 3.1. Ship voyage

Each shipping line allocates a number of ships (q) for service of every shipping route, which is composed of a specific number of ports. Fig. 2 presents a schematic illustration of a hypothetical shipping route with a total of 6 ports of call that is serviced by 4 ships. Let  $P = \{1, ..., a\}$  denote a set of ports for a given shipping route. Each ship should visit every port of the shipping route throughout its voyage. The sailing path amongst two ports of a shipping route is called a "voyage leg". Each ship in the shipping line's fleet sails from port p to port p along voyage leg p. Import containers are unloaded from ships at the ports of a shipping route, while export containers are loaded on board the ships. After serving the last port (i.e., port "6" in the provided example), each ship returns to the first port of call (i.e., port "1" in the provided example).

## 3.2. Fuel consumption modeling

Accurate fuel consumption modeling is essential for the ship schedule design, as the fuel consumption cost may comprise a substantial portion of the total shipping route service cost (Ronen, 2011; Wang and Meng, 2012). There are many different operational and physical factors that may influence the fuel consumption by the main ship engines that turn the propellers. These factors include, but are not solely limited to, age of the ship, geometry of the ship, propeller design,

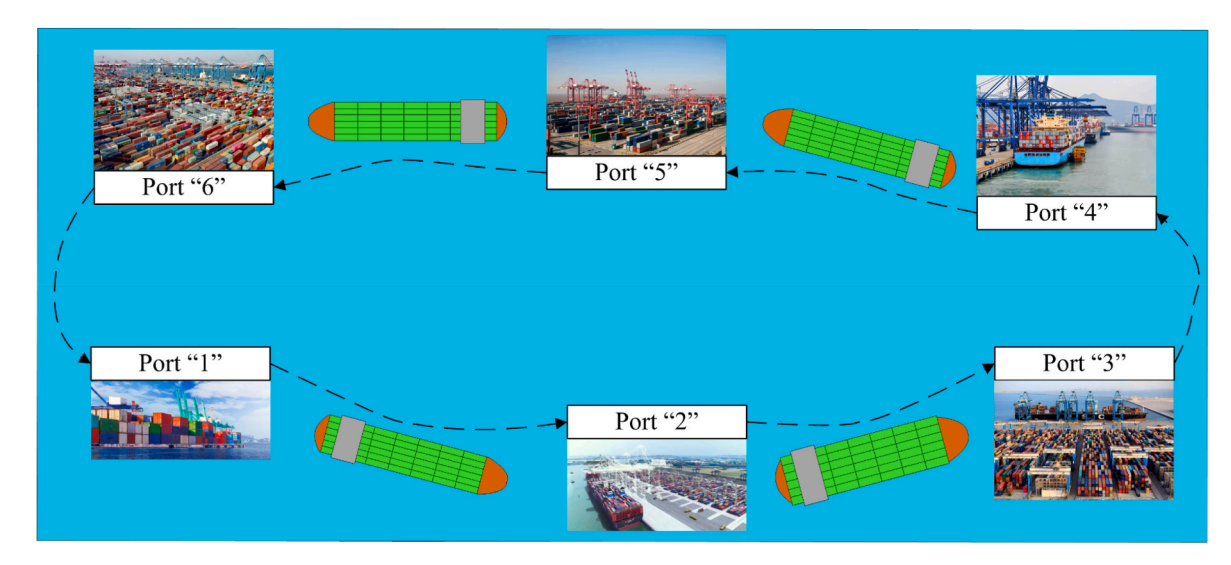


Fig. 2. Schematic illustration of a hypothetical shipping route.

previous maintenance activities, previous repairs, payload, and weather conditions (Psaraftis and Kontovas, 2013; Wang and Meng, 2017). The ship sailing speed is viewed as the most influential predictor for the ship fuel consumption (Wang and Meng, 2012; Pasha et al., 2021). Therefore, the design fuel consumption by the main ship engines at voyage leg p ( $\varphi_D^{design}$ ,  $p \in P$  – tons/nmi) can be computed using the following equation:

$$\varphi_p^{design} = \frac{\gamma(s_p)^{\alpha-1}}{24} \,\forall p \in P \tag{3-1}$$

where:  $s_p, p \in P$  – ship sailing speed to be set at voyage leg p (knots);  $\alpha, \gamma$  – coefficients for the fuel consumption function of the main ship engines.

In the meantime, many studies underline the influence of payload on the fuel consumption of the main ship engines (Psaraftis and Kontovas, 2013; Kontovas, 2014; Pasha et al., 2021). Indeed, fully-laden ships consume more fuel when comparing to partially-laden or ballast ships, especially at higher sailing speeds (Psaraftis and Kontovas, 2013), which further increases the quantity of emissions released by the main ship engines (see Fig. 3). Hence, in order to capture the effects of ship payload, this study uses the following equation for computing the fuel consumption by the main ship engines at voyage leg p ( $\varphi_p, p \in P$  – tons/nmi) based on the design ship fuel consumption (Kontovas, 2014;

Adland and Jia, 2016; Pasha et al., 2021):

$$\boldsymbol{\varphi}_{p} = \boldsymbol{\varphi}_{p}^{design} \cdot \left(\frac{\boldsymbol{\varphi}_{p}^{sea} \cdot \boldsymbol{\varpi} + \boldsymbol{\psi}^{empty}}{\boldsymbol{\psi}^{cap} + \boldsymbol{\psi}^{empty}}\right)^{\frac{2}{3}} = \frac{\boldsymbol{\gamma}(\boldsymbol{s}_{p})^{a-1}}{24} \cdot \left(\frac{\boldsymbol{\varphi}_{p}^{sea} \cdot \boldsymbol{\varpi} + \boldsymbol{\psi}^{empty}}{\boldsymbol{\psi}^{cap} + \boldsymbol{\psi}^{empty}}\right)^{\frac{2}{3}} \forall p \in P$$
(3-2)

where:  $\psi_p^{sea}, p \in P$  – total number of containers (i.e., the ship payload) that will be carried at voyage leg p (TEUs);  $\varpi$  – average cargo weight inside a standard 20-ft container (tons);  $\psi^{empty}$  – empty weight of a ship to be deployed (tons);  $\psi^{cap}$  – total capacity of a ship to be deployed (tons).

When selecting the sailing speed at voyage legs of a given shipping route, the shipping line has to consider certain lower and upper bounds, which will be denoted as  $s^{min}$  (knots) and  $s^{max}$  (knots) in this manuscript, respectively. These bounds are generally determined based on specific practical considerations (e.g., capacity of the main ship engines, potential wear of the main ship engines when sailing at very low speeds) (Psaraftis and Kontovas, 2013; Wang et al., 2013). Note that this study explicitly models the fuel consumption by the main ship engines only. The fuel consumption by the auxiliary ship engines that are responsible for power generation typically does not change substantially throughout the ship voyage (Pasha et al., 2021). Hence, it is accounted for in the ship

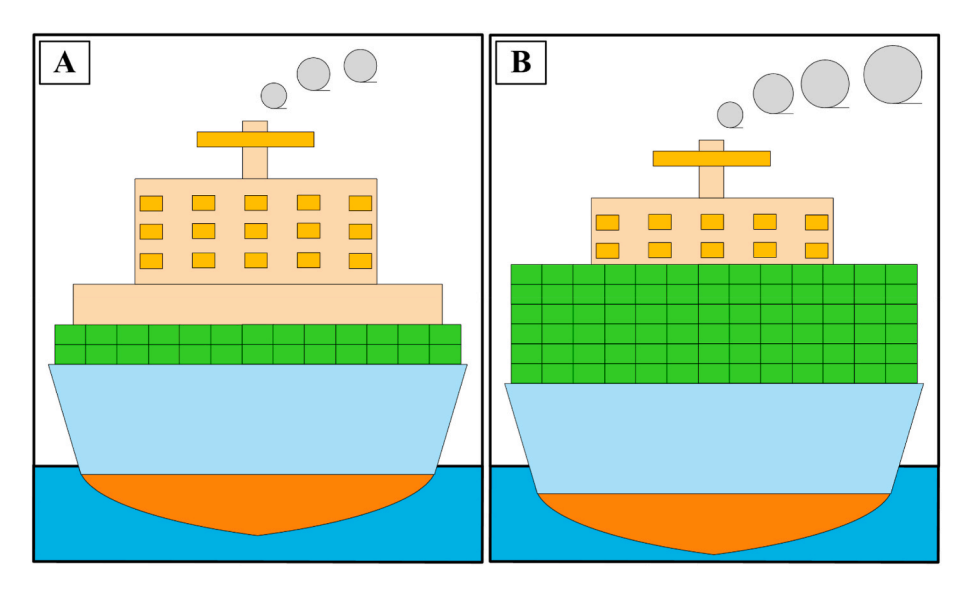


Fig. 3. Schematic illustration of a ship sailing in partially-laden (A) and fully-laden (B) modes.

operational cost or the ship chartering cost in case the additional ships have to be charted from other shipping lines.

#### 3.3. Marine terminal operations and collaborative agreements

As indicated in the introduction section of the manuscript, this study proposes a novel mathematical model that explicitly captures comprehensive collaborative agreements amongst shipping lines and marine terminal operators, where the shipping line is not only able to select the marine terminal for the ship service at every port of the shipping route but also request the appropriate arrival time window and handling rate (see Fig. 1). Let  $M_p = \{1, ..., b_p\}, p \in P$  denote a set of marine terminals available at port p that have collaborative agreements in place and can share the available capacity (i.e., berthing space, arrival time windows, handling equipment, etc.) for service of the arriving ships. A set of ship arrival time windows available at terminal m of port p will be referred to as  $T_{pm} = \{1, ..., c_{pm}\}, p \in P, m \in M_p$ . To allow flexibility of ship schedules, this study adopts the concept of soft time windows, originally introduced by Fagerholt (2001). In particular, the ships are not restricted to arrive within the selected time window and can arrive before the time window start and after the time window end. When a ship arrives before the time window start, it will be required to wait for service, as the available handling resources may be reserved for service of other ships. On the other hand, it is assumed that the ship service can start upon its arrival even if the ship arrived after the time window end. However. an additional cost will be incurred by the shipping line in order to compensate the operator of the selected terminal for the utilization of limited handling resources after the agreed arrival time window.

Depending on the equipment available during time window t, each terminal operator m of port p is able to provide a set of handling rates  $H_{pmt} = \{1, ..., d_{pmt}\}, p \in P, m \in M_p, t \in T_{pm}$ . Every handling rate has a specific handling productivity  $\pi_{pmth}, p \in P, m \in M_p, t \in T_{pm}, h \in H_{pmt}$  that essentially defines the total number of TEUs that can be handled at terminal m of port p during time window t per hour. Index "p" is used in  $\pi_{pmth}$  to capture the variability of container handling resources amongst the ports of a given shipping route, whereas index "m" accounts for the operational feature that even collaborating marine terminals at the same port may have different resources for service of the arriving ships. Furthermore, index "t" is used to model variations of the available capacity (e.g., berthing space) by time of day, as less arrival time windows will be available during peak hours compared to off-peak hours. In the meantime, index "h" captures different handling rates that can be provided by collaborating marine terminals during the available time windows. Considering the aforementioned operational features, the handling time of a ship at port p ( $\tau_p^{hand}$ ,  $p \in P$  – hours) can be computed using the following equation:

$$\boldsymbol{\tau}_{p}^{hand} = \sum_{m \in M} \sum_{t \in T_{-}} \sum_{h \in H_{-}} \left( \frac{\varphi_{p}^{port}}{\pi_{pmth}} \right) \boldsymbol{z}_{pmth} \ \forall p \in P$$
(3-3)

where:  $z_{pmth}, p \in P, m \in M_p, t \in T_{pm}, h \in H_{pmt} = 1$  if handling rate h will be used for the ship service at terminal m of port p during time window t (else = 0);  $\varphi_p^{port}, p \in P$  – total number of containers that will be handled at port p (TEUs).

## 3.4. Port service frequency requirements

Each shipping line has to serve every port of a given shipping route with a particular frequency (e.g., daily, weekly, bi-weekly). This study assumes that every port should be visited on a weekly basis; however, without loss of generality, other service frequency requirements can be captured by the proposed mathematical model as well. The following relationship must be maintained by the sipping line to ensure that every port of the considered shipping route is served on a weekly basis (Alharbi et al., 2015; Pasha et al., 2021):

$$168q = \sum_{n \in P} \tau_p^{vail} + \sum_{n \in P} \tau_p^{hand} + \sum_{n \in P} \tau_p^{wait}$$
 (3-4)

where: "168" – number of hours in a one-week time interval;  $\tau_p^{sail}$ ,  $p \in P$  – sailing time of a ship at voyage leg p (hours);  $\tau_p^{wait}$ ,  $p \in P$  – waiting time of a ship at port p (hours).

The left-hand side of equation (3-4) represents a product of "168" (i. e., number of hours in a one-week time interval) and the total number of ships to be deployed for a given shipping route. The right-hand side of equation (3-4) is the total ship turnaround time, which is the time that takes for each deployed ship to visit every port of a given shipping route and return to the first port after a round voyage. The total ship turnaround time is composed of the total sailing time of ships at voyage legs, total handling time of ships at ports, and total waiting time of ships at ports. The total ship turnaround time can be reduced by increasing the ship sailing speed (that will further decrease the total sailing time at voyage legs) and requesting handling rates with higher handling productivities (that will further decrease the total handling time at ports). However, these actions would cause an increase in the total ship fuel cost and the total ship service cost at ports. Nevertheless, a total ship turnaround time reduction will be favorable in terms of the total ship operating cost, as fewer ships will have to be assigned for service of a given shipping route in order to maintain the weekly service frequency at ports.

In case the total number of own ships available ( $q^{own-max}$  – ships) is not sufficient for service of a given shipping route, the shipping line will have to charter the ships from other shipping lines. The total number of ships available for chartering will be denoted as  $q^{char-max}$  (ships). Hence, the following relationships have to be considered by the shipping line for the total number of own ships deployed ( $q^{own}$  – ships) and for the total number of chartered ships deployed ( $q^{char}$  – ships) in the ship schedule design:

$$q = q^{own} + q^{char} \tag{3-5}$$

$$q^{own} \le q^{own-max} \tag{3-6}$$

$$q^{char} \le q^{char - max} \tag{3-7}$$

The cost of ship chartering is generally higher than the cost of operating own ships, which may further increase the total shipping route service cost. In case the total cost of ship charting becomes substantial, the shipping line may decide to increase the sailing speed of own ships. Such a strategy could allow maintaining the agreed weekly port service frequency without deploying any chartered ships.

# 3.5. Container inventory throughout the ship voyage

Slow steaming (i.e., sailing at low speeds) has been widely used by shipping lines to reduce the ship fuel consumption and the associated fuel costs along with the total quantity of emissions released (De et al., 2016; Wen et al., 2017; Mallidis et al., 2018). Slow steaming has some disadvantages as well, since a reduction in the ship sailing speed will inevitably lead to increasing total ship sailing time and the amount of time the containers will spend on board the ships. Excessive amount of time that the containers spend on ships negatively affects the shipping efficiency and is not viewed as desirable by customers. Therefore, the total container inventory cost should be directly accounted for by the shipping line in the ship schedule design. The total container inventory cost ( $A^{inv}$  – USD) can be computed based on the unit cost of container inventory ( $\delta^{inv}$  – USD per TEU per hour), total number of containers (i.e., the ship payload) that will be carried at voyage  $\log p$  ( $\varphi_p^{sea}, p \in P$  – TEUs), and total sailing time of ships at voyage legs ( $au_p^{sail}, p \in P$  – hours) using the following equation (Wang et al., 2014; Pasha et al., 2021):

$$\Lambda^{inv} = \delta^{inv} \sum_{p \in P} \varphi_p^{sea} \tau_p^{seal}$$
 (3-8)

#### 3.6. Emission modeling

As indicated earlier in the introduction section, the IMO continues imposing more and more restrictions on oceangoing ships to reduce the quantity of emissions released. In order to meet the IMO environmental targets, shipping lines have to directly account for the amount of emissions produced by ships when sailing along the voyage legs in the ship schedule design. The fourth IMO study on greenhouse gas emissions classifies the emissions produced by oceangoing ships into two major classes, including the following (IMO, 2020): (i) greenhouse gas emissions; and (ii) other relevant substances. Greenhouse gas emissions are mostly represented by carbon dioxide – CO<sub>2</sub>, methane – CH<sub>4</sub>, and nitrous oxide – N<sub>2</sub>O. Other relevant substances include nitrogen oxides – NO<sub>x</sub>, sulfur oxides - SO<sub>x</sub>, carbon monoxide - CO, non-methane volatile organic compounds - VOC, particulate matter - PM, and black carbon -BC. The most common method for estimating emissions produced by oceangoing ships that has been widely used in the ship scheduling literature is based on the emission factors (Psaraftis and Kontovas, 2013; Kontovas, 2014). In particular, each pollutant is assumed to have a certain emission factor, which is measured in the total quantity of emissions released per ton of fuel burned. Hence, the total amount of emissions that will be produced at voyage leg p ( $\xi_p^{sea}, p \in P$  – tons) can be computed using the following equation:

$$\boldsymbol{\xi}_{p}^{sea} = \eta^{sea} \lambda_{p} \boldsymbol{\varphi}_{p} \ \forall p \in P \tag{3-9}$$

where:  $\eta^{sea}$  – emission factor at sea for a given pollutant (tons of emissions/ton of fuel);  $\lambda_p$  – length of voyage leg p (nmi).

The emission factor at sea ( $\eta^{sea}$ ) may significant vary for different pollutants. For example, the emission factor for  $CO_2$  comprises 3.144 tons of  $CO_2$  emissions/ton of fuel, whereas the emission factor for  $NO_x$  comprises 78.61 kg of  $NO_x$  emissions/ton of fuel (Kontovas, 2014; IMO, 2020). Along with the emissions produced at sea, the amount of emissions released at ports by the designated container handling equipment has to be accounted for by the shipping line in the ship schedule design as well. Similar to the emissions produced at sea, the total amount of emissions that will be produced by the designated container handling equipment at port p ( $\xi_p^{port}$ ,  $p \in P$  – tons) can be computed based on the emission factors using the following equation (Tran et al., 2017):

$$\boldsymbol{\xi}_{p}^{port} = \boldsymbol{\varphi}_{p}^{port} \sum_{m \in M_{pt} \in T_{pm}} \sum_{h \in H_{pmt}} \boldsymbol{\eta}_{pmth}^{port} \boldsymbol{z}_{pmth} \, \forall p \in P$$
(3-10)

where:  $\eta_{pmth}^{port}$  – emission factor for the ship service under handling rate h at terminal m of port p during time window t (tons of emissions/TEU).

According to Tran et al. (2017), the emission factor for  $CO_2$  due to cargo handling operations at ports  $(\eta_{pmth}^{port}, p \in P, m \in M_p, t \in T_{pm}, h \in H_{pmt})$  is approximately 17.29 kg of  $CO_2$  per TEU (assuming the base handling productivity of 180 TEU/hour). From the practical point of view, the amount of emissions produced by the designated container handling equipment will not be affected just by the handling rate requested but also by the type of container handling equipment deployed by the marine terminal operator at a given port during the selected time window (e.g., during a peak-hour period, the marine terminal operator at a given port may have only certain types of container handling equipment available). Therefore, along with index "h", the term " $\eta_{pmth}^{port}$ " includes indexes "p", "m", and "t".

### 4. Mathematical model development

#### 4.1. Nomenclature

#### Sets

$P = \{1,, a\}$	set of ports for a given shipping route
$ extbf{ extit{M}}_{ extit{p}} = \{1,,b_{ extit{p}}\},  extit{p} \in  extit{P}$	set of marine terminals available at port p
$T_{pm} = \{1,,c_{pm}\}, p \in P,$	set of ship arrival time windows available at terminal $m$
$m \in M_p$	of port p
$H_{pmt} = \{1,,d_{pmt}\}, p \in P,$	set of handling rates available at terminal $m$ of port $p$ during time window $t$
$m \in M_p, t \in T_{pm}$	

#### Decision variables

$s_p \in \mathbb{R}^+ \ orall p \in P$	ship sailing speed to be set at voyage $leg p$ (knots)
$x_{pm} \in \mathbb{B} \ \forall p \in P, m \in$	= 1 if terminal $m$ will be used for the ship service at port $p$
$M_p$	(else = 0)
$y_{pmt} \in \mathbb{B} \ \forall p \in P, m \in$	t=1 if time window $t$ will be used for the ship service at
$M_p$ ,	terminal $m$ of port $p$ (else = 0)
$t \in T_{pm}$	
$z_{pmth} \in \mathbb{B} \ \forall p \in P, m \in$	= 1 if handling rate $h$ will be used for the ship service at
$M_p$ ,	terminal $m$ of port $p$ during time window $t$ (else = 0)
$t \in T_{pm}, h \in H_{pmt}$	

## Auxiliary variables

$q\in\mathbb{N}$	total number of ships for deployment (ships)
$q^{own} \in \mathbb{N}$	total number of own ships for deployment (ships)
$q^{char} \in \mathbb{N}$	total number of chartered ships for deployment (ships)
$ au_p^{arr} \in \mathbb{R}^+ \ orall p \in P$	arrival time of a ship at port $p$ (hours)
$ au_p^{wait} \in \mathbb{R}^+ \ orall p \in P$	waiting time of a ship at port $p$ (hours)
$ au_p^{hand} \in \mathbb{R}^+ \ orall p \in P$	handling time of a ship at port $p$ (hours)
$ au_p^{dep} \in \mathbb{R}^+ \ orall p \in P$	departure time of a ship from port $p$ (hours)
$ au_p^{sail} \in \mathbb{R}^+ \ orall p \in P$	sailing time of a ship at voyage $leg p$ (hours)
$oldsymbol{arphi}_p \in \mathbb{R}^+ \ orall p \in P$	fuel consumption of a ship at voyage $leg\ p$ (tons/nmi)
$ au_p^{late} \in \mathbb{R}^+ \ orall p \in P$	late arrival of a ship at port $p$ (hours)
$oldsymbol{\xi}_p^{sea} \in \mathbb{R}^+ \ orall p \in P$	total amount of emissions that will be produced at voyage $\log p$ (tons)
$oldsymbol{\xi}_p^{port} \in \mathbb{R}^+ \ orall p \in P$	total amount of emissions that will be produced at port $p$ (tons)
$\Lambda^{own} \in \mathbb{R}^+$	total operational cost of own ships (USD)
$oldsymbol{arLambda^{char}} \in \mathbb{R}^{+}$	total cost of ship chartering (USD)
$\mathbf{\Lambda}^{inv} \in \mathbb{R}^+$	total cost of container inventory (USD)
$\mathbf{\Lambda}^{late} \in \mathbb{R}^+$	total cost of ship late arrival at ports (USD)
$\Lambda^{\mathit{fuel}} \in \mathbb{R}^+$	total cost of ship fuel (USD)
$\mathbf{\Lambda}^{port} \in \mathbb{R}^+$	total cost of ship service at ports (USD)
$\Lambda^{emis} \in \mathbb{R}^+$	total cost of ship emissions (USD)

# Parameters

$a \in \mathbb{N}$	total number of ports under a given port rotation (ports)
$b_p \in \mathbb{N} \ \forall p \in P$	total number of marine terminals available at port $p$
	(ports)
$c_{pm} \in \mathbb{N} \ \forall p \in P, m \in M_p$	total number of ship arrival time windows available at
	terminal $m$ of port $p$ (time windows)
$d_{pmt} \in \mathbb{N} \ \forall p \in P, m \in$	total number of handling rates available at terminal $\boldsymbol{m}$ of
$M_p$ ,	port p during time window t (rates)
$t \in T_{pm}$	
$\alpha, \gamma \in \mathbb{R}^+$	coefficients for ship fuel consumption
$oldsymbol{arpi} \in \mathbb{R}^+$	average cargo weight inside a standard 20-ft container
	(tons)
$\psi^{empty} \in \mathbb{R}^+$	empty weight of a ship to be deployed (tons)
$\psi^{cap} \in \mathbb{R}^+$	total capacity of a ship to be deployed (tons)
$\eta^{sea} \in \mathbb{R}^+$	emission factor at sea (tons of emissions/ton of fuel)
$\eta_{pmth}^{port} \in \mathbb{R}^+ \ \forall p \in P$ ,	emission factor for the ship service under handling rate $\boldsymbol{h}$
$m \in M_p, t \in T_{pm}, h \in$	at terminal $m$ of port $p$ during time window $t$ (tons of
$H_{pmt}$	emissions/TEU)
$\pi_{pmth} \in \mathbb{R}^+ \ \forall p \in P,$	handling productivity for handling rate $\boldsymbol{h}$ that will be used
$m \in M_n, t \in T_{nm}, h \in$	for the ship service at terminal <i>m</i> of port <i>p</i> during time

window t (TEUs/hour)

(continued on next page)

#### (continued)

$\delta^{own} \in \mathbb{R}^+$	weekly operational cost of own ships (USD/week)
$\delta^{char} \in \mathbb{R}^+$	weekly cost of ship chartering (USD/week)
$\delta^{inv} \in \mathbb{R}^+$	unit cost of container inventory (USD per TEU per hour)
$\delta_p^{\mathit{late}} \in \mathbb{R}^+ \ orall p \in P$	unit cost of ship late arrival at port $p$ (USD/hour)
$\delta_p^{fuel} \in \mathbb{R}^+$	unit cost of ship fuel at voyage $leg p$ (USD/ton)
$\delta_{pmth}^{hand} \in \mathbb{R}^+ \ orall p \in P,$	unit cost of ship service under handling rate $\boldsymbol{h}$ at terminal
$m \in M_p, t \in T_{pm}, h \in$	m of port $p$ during time window $t$ (USD/TEU)
$H_{pmt}$	
$\delta^{emis} \in \mathbb{R}^+$	unit cost of ship emissions (USD/ton)
$\lambda_p \in \mathbb{R}^+ \ orall p \in P$	length of voyage $leg p$ (nmi)
$arphi_p^{sea} \in \mathbb{N} \ orall p \in P$	total number of containers that will be carried at voyage
•	leg p (TEUs)
$arphi_p^{port} \in \mathbb{N} \ orall p \in P$	total number of containers that will be handled at port $p$ (TEUs)
$s^{min} \in \mathbb{R}^+$	lower bound on ship sailing speed (knots)
$s^{max} \in \mathbb{R}^+$	upper bound on ship sailing speed (knots)
$q^{own-max} \in \mathbb{N}$	available number of own ships for deployment (ships)
$q^{char-max} \in \mathbb{N}$	available number of chartered ships for deployment
	(ships)
$ au_{pmt}^{st} \in \mathbb{R}^+ \ orall p \in P, m \in$	start time for time window $t$ at terminal $m$ of port $p$ (hours)
$M_p$ ,	
$t \in T_{pm}$	
$ au_{pmt}^{end} \in \mathbb{R}^+ \ orall p \in P, m \in$	end time for time window $t$ at terminal $m$ of port $p$ (hours)
$M_p$ ,	
$t \in T_{pm}$	

#### 4.2. Model formulation

A bi-objective mixed-integer programming model for a ship scheduling problem with collaborative agreements amongst the shipping line and marine terminal operators (SSP-CAT) can be formulated as follows. The first objective function  $(F_1)$  aims to minimize the cost components that are mostly driven by the economic perspectives, including the following: (i) the total operational cost of own ships; (ii) the total cost of ship chartering; (iii) the total cost of container inventory; and (iv) the total cost of ship late arrival at ports. On the other hand, the second objective function  $(F_2)$  aims to minimize the cost components that are driven not only by the economic perspectives but also by the environmental perspectives as well and include the following: (i) the total cost of ship fuel; (ii) the total cost of ship service at ports; and (iii) the total cost of ship emissions.

$$min F_1 = \left[ \Lambda^{own} + \Lambda^{char} + \Lambda^{inv} + \Lambda^{late} \right]$$
 (4-1)

$$min F_2 = \left[ \Lambda^{fuel} + \Lambda^{port} + \Lambda^{emis} \right] \tag{4-2}$$

Indeed, the objective functions  $F_1$  and  $F_2$  are conflicting in nature. If a shipping line decides to strictly pursue the environmental sustainability goals, it will set the lowest possible sailing speed for the available ships to reduce the fuel consumption and the associated emissions produced by ships at sea. Furthermore, the shipping line will select the lowest possible handing rates at the ports of shipping route to reduce the associated emissions produced by the designated handling equipment throughout the service of arriving ships. The aforementioned actions will reduce the  $F_2$  objective. However, decreasing sailing speed of ships and handing rates at ports will increase the amount of time spent at sea and ports, respectively. Therefore, the total turnaround time of ships will increase as well, which will necessitate the deployment of additional own ships and/or chartered ships to ensure that the weekly port service frequency is maintained. Moreover, decreasing sailing speed of ships and handing rates at ports will increase the total cost of container inventory (as containers will have to stay longer on board the ships) and is likely to cause late ship arrivals at ports. Hence, a decrease in the  $F_2$ objective is likely to increase the  $F_1$  objective. Note that both objective functions  $F_1$  and  $F_2$  of the SSP-CAT mathematical model are costrelated, and the unit costs of objective components (i.e.,  $\delta^{own}$ ,  $\delta^{char}$ ,  $\delta^{inv}$ ,  $\delta_p^{late}$ ,  $\delta_p^{fuel}$ ,  $\delta_p^{hand}$ , and  $\delta_p^{emis}$ ) play the role of normalizing coefficients. The

normalizing coefficients are necessary for computing the objective function components (e.g., the total fuel consumption, measured in tons of fuel, cannot be added to the total amount of emissions, measured in tons of emissions, without applying normalizing coefficients).

A number of operational constraints are directly captured by the SSP-CAT mathematical model, which can be divided into the following six groups. The first constraint group, which is represented by constraints (4-3)-(4-7), focuses on the main operations at the ports of shipping route. More specifically, constraints (4-3) guarantee that only one marine terminal will be selected for the ship service at every port of the shipping route. Constraints (4-4) and (4-5) enforce the condition that only one time window will be chosen for the ship service at the selected terminal of every port. On the other hand, constraints (4-6) and (4-7) enforce the condition that only one handling rate will be used for the ship service during the selected time window and terminal of every port.

$$\sum_{m \in M_n} \mathbf{x}_{pm} = 1 \ \forall p \in P \tag{4-3}$$

$$\sum_{m \in M_{pl} \in T_{pm}} \mathbf{y}_{pml} = 1 \ \forall p \in P$$
 (4-4)

$$\mathbf{y}_{pmt} \le \mathbf{x}_{pm} \ \forall p \in P, m \in M_p, t \in T_{pm}$$

$$\tag{4-5}$$

$$\sum_{m \in \mathcal{M}_{p} \in \mathcal{T}_{pm}} \sum_{h \in \mathcal{H}_{mnt}} z_{pmth} = 1 \ \forall p \in P$$

$$\tag{4-6}$$

$$\mathbf{z}_{pmth} \leq \mathbf{y}_{pmt} \ \forall p \in P, m \in M_p, t \in T_{pm}, h \in H_{pmt}$$

$$\tag{4-7}$$

The second constraint group, which is represented by constraints (4-8) and (4-9), captures the ship sailing speed limitations and estimates the required amount of ship fuel. In particular, constraints (4-8) ensure that the selected ship sailing speed will not be less than its lower bound and will not go beyond its upper bound. Constraints (4-9) compute the required amount of ship fuel at every voyage leg based on the selected ship sailing speed as well as the ship payload.

$$s^{min} \le s_p \le s^{max} \ \forall p \in P \tag{4-8}$$

$$\boldsymbol{\varphi}_{p} = \frac{\gamma(\boldsymbol{s}_{p})^{\alpha-1}}{24} \cdot \left(\frac{\boldsymbol{\varphi}_{p}^{sea} \cdot \boldsymbol{\varpi} + \boldsymbol{\psi}^{empty}}{\boldsymbol{\psi}^{cap} + \boldsymbol{\psi}^{empty}}\right)^{\frac{2}{3}} \forall p \in P$$
(4-9)

The third constraint group estimates the total quantity of emissions released by the main ship engines at the voyage legs of shipping route (constraints (4-10)) and the total quantity of emissions released by the designated handling equipment during the service of arriving ships at ports (constraints (4-11)).

$$\boldsymbol{\xi}_{p}^{sea} = \eta^{sea} \lambda_{p} \boldsymbol{\varphi}_{p} \forall p \in P \tag{4-10}$$

$$\boldsymbol{\xi}_{p}^{port} = \boldsymbol{\varphi}_{p}^{port} \sum_{m \in M_{pt} \in T_{pm}} \sum_{h \in H_{pmt}} \boldsymbol{\eta}_{pmth}^{port} \boldsymbol{z}_{pmth} \ \forall p \in P$$

$$\tag{4-11}$$

The fourth constraint group, which is represented by constraints (4-12)-(4-19), computes certain important time components that are directly used by the shipping line in the ship schedule design, including the following: (i) sailing time of ships at every voyage leg (constraints (4-12)); (ii) arrival time of ships at every port (constraints (4-13) and (4-14)); (iii) late arrivals of ships at every port (constraints (4-15)); (iv) waiting time of ships at every port (constraints (4-16) and (4-17)); (v) handling time of ships at every port (constraints (4-18)); and (vi) departure time of ships from every port (constraints (4-19)).

$$\boldsymbol{\tau}_{p}^{sail} = \frac{\lambda_{p}}{\mathbf{s}_{p}} \ \forall p \in P$$
 (4-12)

$$\boldsymbol{\tau}_{(p+1)}^{arr} = \boldsymbol{\tau}_p^{dep} + \boldsymbol{\tau}_p^{vail} \ \forall p \in P, p < \left| \boldsymbol{P} \right| \tag{4-13}$$

$$\boldsymbol{\tau}_{1}^{arr} = \boldsymbol{\tau}_{p}^{dep} + \boldsymbol{\tau}_{p}^{sail} - 168\boldsymbol{q} \ \forall p \in P, p = \left| P \right|$$
 (4-14)

$$\boldsymbol{\tau}_{p}^{late} \geq \boldsymbol{\tau}_{p}^{arr} - \sum_{m \in M, t \in T_{om}} \boldsymbol{\tau}_{pmt}^{end} \boldsymbol{y}_{pmt} \ \forall p \in P$$

$$\tag{4-15}$$

$$\boldsymbol{\tau}_{(p+1)}^{wait} \ge \sum_{m \in M_{p}} \sum_{t \in T_{pm}} \boldsymbol{\tau}_{(p+1)mt}^{st} \boldsymbol{y}_{(p+1)mt} - \boldsymbol{\tau}_{p}^{dep} - \boldsymbol{\tau}_{p}^{sail} \ \forall p \in P, p < \left| P \right|$$

$$(4-16)$$

$$\boldsymbol{\tau}_{1}^{wait} \geq \sum_{m \in M_{p} t \in T_{pm}} \boldsymbol{\tau}_{1mt}^{st} \boldsymbol{y}_{1mt} - \boldsymbol{\tau}_{p}^{dep} - \boldsymbol{\tau}_{p}^{sail} + 168\boldsymbol{q} \ \forall p \in P, p = \left| P \right|$$

$$(4-17)$$

$$\boldsymbol{\tau}_{p}^{hand} = \sum_{m \in \mathcal{M}} \sum_{s \in \mathcal{T}} \sum_{h \in \mathcal{H}} \left( \frac{\boldsymbol{\varphi}_{p}^{port}}{\boldsymbol{\pi}_{pmth}} \right) \boldsymbol{z}_{pmth} \ \forall p \in P$$
 (4-18)

$$\boldsymbol{\tau}_{p}^{dep} = \boldsymbol{\tau}_{p}^{arr} + \boldsymbol{\tau}_{p}^{wait} + \boldsymbol{\tau}_{p}^{hand} \ \forall p \in P$$
 (4-19)

The fifth constraint group, which is represented by constraints (4-20)-(4-23), ensures that the target frequency of port service is maintained for the given shipping route. More specifically, constraints (4-20) enforce the condition that every port is visited exactly once a week. Constraints (4-21) calculate the total number of own and chartered ships necessary for providing weekly service frequency at ports. Constraints (4-22) and (4-23) guarantee that the total number of own and chartered ships will not go beyond the available number of own and chartered ships, respectively.

$$168q = \sum_{p \in P} \tau_p^{\text{vail}} + \sum_{p \in P} \tau_p^{\text{hand}} + \sum_{p \in P} \tau_p^{\text{wait}}$$
 (4-20)

$$q = q^{own} + q^{char} \tag{4-21}$$

$$q^{own} \le q^{own-max} \tag{4-22}$$

$$q^{char} \le q^{char-max} \tag{4-23}$$

The sixth constraint group, which is represented by constraints (4-24)-(4-30), estimates the individual cost components that are directly used for computing objective functions  $F_1$  and  $F_2$  of the SSP-CAT mathematical model.

$$\Lambda^{own} = \delta^{own} q^{own} \tag{4-24}$$

$$\Lambda^{char} = \delta^{char} q^{char} \tag{4-25}$$

$$\Lambda^{inv} = \delta^{inv} \sum_{p \in P} \varphi_p^{vea} \tau_p^{vail} \tag{4-26}$$

$$\Lambda^{late} = \sum_{p \in P} \delta_p^{late} \tau_p^{late} \tag{4-27}$$

$$\boldsymbol{\Lambda}^{fuel} = \sum_{p \in P} \lambda_p \delta_p^{fuel} \boldsymbol{\varphi}_p \tag{4-28}$$

$$\Lambda^{port} = \sum_{p \in P} \sum_{m \in M} \sum_{l \in T_{m,p}} \sum_{h \in H_{m,m}} \varphi_p^{port} \delta_{pmth}^{hand} z_{pmth}$$

$$(4-29)$$

$$\Lambda^{emis} = \delta^{emis} \sum_{p \in P} \left( \xi_p^{sea} + \xi_p^{port} \right) \tag{4-30}$$

# 5. Solution methodology

#### 5.1. Model linearization

The computational complexity of the original SSP-CAT model can be reduced through the application of linearization techniques. First, the ship sailing speed reciprocal  $s_p^r = 1/s_p \ \forall p \in P \ (\mathrm{knots^{-1}})$  can be used as a substitute of the ship sailing speed. Second, a continuous non-linear ship fuel consumption function  $\varphi_p, p \in P \ (\mathrm{tons/nmi})$  can be transformed into a set of discrete points  $K = \{1, ..., e\}$ . Let  $s_k^{val}, k \in K \ (\mathrm{knots^{-1}})$  be the reciprocal value of ship sailing speed for discrete point k, and  $\varphi_k^{val}, k \in K \ (\mathrm{tons/nmi})$  be the design ship fuel consumption estimated using the reciprocal of ship sailing speed for discrete point k. Assume  $\beta_{pk}$  to be 1 if discrete point k is used to estimate the value of ship fuel consumption at voyage leg p (else = 0). The original mixed integer non-linear multiobjective SSP-CAT model can be then presented in a linearized form as follows:

SSP-CATL: Linearized Ship Scheduling Problem with Collaborative Agreements amongst the Shipping Line and Marine Terminal Operators

The objective functions  $F_1$  and  $F_2$  aim to minimize the conflicting

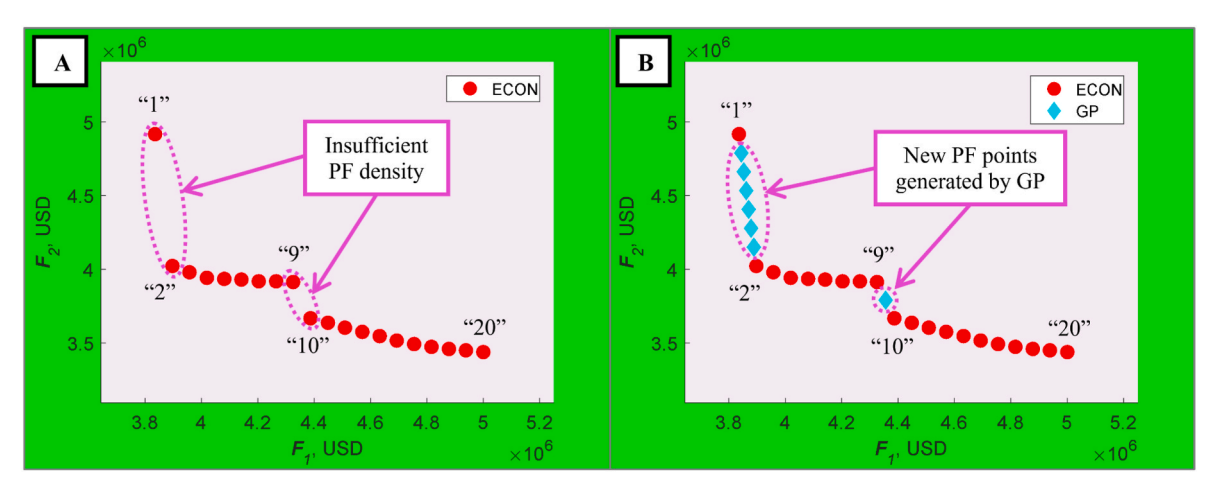


Fig. 4. Basic principles behind the proposed ECON-GP method.

costs of the SSP-CATL model. Constraints (5-3) assure that one discrete point is used to estimate the value of ship fuel consumption at every voyage leg. Constraints (5-4) calculate the reciprocal value of ship sailing speed by using the discrete point selected at every voyage leg. Constraints (5-5) compute the ship fuel consumption by using the discrete point selected at every voyage leg and directly considering the ship payload. Constraints (5-6) calculate the ship sailing time at every voyage leg. Constraints (5-7) impose bounds on the reciprocal value of ship sailing speed.

## 5.2. Exact multi-objective optimization approach

A variety of metaheuristic-based algorithms have been used for complex multi-objective optimization problems (e.g., NSGA-I, NSGA-II, SPEA-I, SPEA-II, MOKA, MOBSO, etc.) (Fathollahi-Fard et al., 2018, 2021). However, single-objective ship schedule design problems can be generally tackled using exact optimization methods within an acceptable amount of computational time (Dulebenets, 2018; Pasha et al., 2020). Therefore, this study proposes a novel customized exact multi-objective optimization approach to solve the SSP-CATL model, which is inspired by two well-known algorithms, the ε-constraint method (ECON) and the goal programming method (GP), and will be further referred to as ECON-GP. The ECON method minimizes one

objective of the optimization model (generally, the most important one from the practical point of view) and imposes bound(s) on the other objective function(s) (Mavrotas, 2009). The Pareto Front (PF) is developed by iteratively changing the bound values. On the other hand, the GP method sets certain target values for the considered objectives of the optimization model, aiming to minimize the total deviation of the objective values from the established target values (Deb. 1999). Both ECON and GP have some limitations. In particular, the ECON method may generate a PF with insufficient density. Fig. 4A shows an example PF with 20 points, where evenly-spaced bounds are imposed on the objective  $F_1$ . However, after solving the optimization model and minimizing the objective  $F_2$  (while iteratively imposing certain bounds on the objective  $F_1$ ), the distance amongst some of the consecutive PF points in terms of the  $F_2$  interval is significant, which causes the insufficient PF density (i.e., the distance amongst points "1" and "2" as well as the distance amongst points "9" and "10"). As for the GP method, one of the main GP limitations consists in the fact that it may be difficult to know the accurate target values for the considered objectives a priori in some instances, and the obtained solutions will have the objective function values that are significantly different from their target values.

Algorithm 1. Hybrid  $\epsilon$ -Constraint and Goal Programming Algorithm (ECON-GP)

```
ECON-GP(InputData, PF^{size}, \varepsilon_1, \varepsilon_2, GP^{tol}, \delta^{F_1}, \delta^{F_2})

in: InputData - the SSP-CATL input data; PF^{size} - PF size; \varepsilon_1 - upper bound on F_1; \varepsilon_2 - upper bound on F_2; GP^{tol} - the GP tolerance value; \delta^{F_1} - penalty for F_1 violation; \delta^{F_2} - penalty for F_2 violation out: PF - PF for the SSP-CATL model

0: PF \leftarrow ECON(InputData, PF^{size}, \varepsilon_1, \varepsilon_2)

\triangleleft Apply ECON to generate the initial PF
```

```
2: while-1 iter \le (PF^{size} - 1) do
3: \Delta \leftarrow PF(iter + 1,2) - PF(iter,2) \triangleleft Estimate the F_2 interval
4: iter \leftarrow iter + 1 \triangleleft Update the iteration counter
```

Algorithm 1: Hybrid \(\varepsilon\)-Constraint and Goal Programming Algorithm (ECON-GP)

6:  $iter_1 \leftarrow 1$   $\triangleleft$  Start the iteration counter

7: while-2  $iter_1 \leq (PF^{size} - 1)$  do

8: **if**  $\Delta(iter_1) > GP^{tol} \cdot mean(\Delta)$  **then**  $\triangleleft$  Check whether the desired PF density is achieved

9:  $PF^{add} \leftarrow \Delta(iter_1)/[GP^{tol} \cdot mean(\Delta)]$   $\triangleleft$  Determine the required number of additional PF points

10:  $\Delta F_1 \leftarrow [PF(iter_1 + 1,1) - PF(iter_1,1)]/PF^{add}$   $\triangleleft$  Determine the  $F_1$  interval amongst the new points

11:  $\Delta F_2 \leftarrow [PF(iter_1 + 1,2) - PF(iter_1,2)]/PF^{add}$   $\triangleleft$  Determine the  $F_2$  interval amongst the new points

12:  $iter_2 \leftarrow 1$   $\triangleleft$  Start the iteration counter

13: **while-3**  $iter_2 \leq (PF^{add} - 1)$  **do** 

14:  $F_1^{target} \leftarrow PF(iter_1, 1) + \Delta F_1 \cdot iter_2$   $\triangleleft$  Estimate the  $F_1$  target value

15:  $F_2^{target} \leftarrow PF(iter_1, 2) + \Delta F_2 \cdot iter_2$   $\triangleleft$  Estimate the  $F_2$  target value

16:  $[\mathbf{F}_1^{GP}; \mathbf{F}_2^{GP}] \leftarrow \mathbf{GP}(InputData, \mathbf{F}_1^{target}, \mathbf{F}_2^{target}, \delta^{F_1}, \delta^{F_2})$   $\triangleleft$  Apply GP to generate the new PF point

17:  $PF \leftarrow PF \cup [F_1^{GP}; F_2^{GP}]$   $\triangleleft$  Append the additional PF point to the PF

18:  $iter_2 \leftarrow iter_2 + 1$   $\triangleleft$  Update the iteration counter

19: **end while-3** 

20: **end if** 

1:  $iter \leftarrow 1$ 

5: end while-1

21:  $iter_1 \leftarrow iter_1 + 1$   $\triangleleft$  Update the iteration counter

22: **end while-2** 

23: return PF

The proposed ECON-GP method relies on the basic features of the ECON and GP methods and effectively addresses the aforementioned limitations of both methods. A detailed description of the main ECON-GP steps is provided in Algorithm 1. First, ECON-GP solves a given multi-objective optimization problem by using the canonical ECON method, where one of the objectives is optimized, while a certain bound is imposed on another objective (step 0 in Algorithm 1). The PF is developed by iteratively changing the bound of the other objective until the desired number of PF points is obtained (see Fig. 4A, where the objective  $F_2$  is minimized, and evenly-spaced bounds are imposed on the objective  $F_1$ ). In the considered example, a total of 20 PF points were generated after applying the ECON method and following the steps outlined in Algorithm 2.

Algorithm 2. ε-Constraint Method (ECON)

"2" and the  $F_2$  interval amongst PF points "9" and "10" exceed the predetermined threshold. Hence, the GP method is used for those intervals to generate additional points and ensure the desirable PF density (see Fig. 4B). The target values for the objectives required by the GP method can be set by means of interpolation amongst the points that have excessive objective intervals (steps 9–19 in Algorithm 1).

The ECON-GP method and the traditional ECON method iteratively solve certain optimization models throughout their execution, including the following: (i) the GP model solved in step 16 of Algorithm 1; (ii) the SSP-CATL-1 model solved in step 1 of Algorithm 2; and (iii) the SSP-CATL-2 model solved in step 2 of Algorithm 2). The GP mathematical model, aiming to minimize the total penalty due to positive and negative deviations of the objective functions  $F_1$  and  $F_2$  (denoted as  $\Delta F_1^+$ ,  $\Delta F_1^-$ ,  $\Delta F_2^+$ , and  $\Delta F_2^-$ , respectively) from their target values (denoted as  $F_1^{target}$ and  $F_2^{target}$ , respectively), can be formulated using additional equations (5-8)-(5-12). Note that parameters  $\delta^{F_1}$  and  $\delta^{F_2}$  represent the penalty values for the deviations of the objective functions  $F_1$  and  $F_2$ , respec-

```
Algorithm 2: ε-Constraint Method (ECON)
```

```
\overline{ECON}(InputData, PF^{size}, \varepsilon_1, \varepsilon_2)
in: InputData - the SSP-CATL input data; PF^{size} - PF size; \varepsilon_1 - upper bound on F_1; \varepsilon_2 - upper bound on F_2
out: PF - PF for the SSP-CATL model
  0: |PF| \leftarrow PF^{size}

⊲ Initialization

  1: [\mathbf{F_1}^*; \mathbf{F_2}(\mathbf{F_1}^*)] \leftarrow \mathbf{SSP\text{-}CATL\text{-}1}(InputData, \varepsilon_2)
                                                                                 \triangleleft Determine the F_1^* corner point
  2: [\mathbf{F}_1(\mathbf{F}_2^*); \mathbf{F}_2^*] \leftarrow \mathbf{SSP\text{-}CATL\text{-}2}(InputData, \varepsilon_1)
                                                                                         \triangleleft Determine the F_2^* corner point
  3: \varepsilon \leftarrow (\mathbf{F}_1(\mathbf{F}_2^*) - \mathbf{F}_1^*)/(PF^{size} - 1)
                                                                     \triangleleft Calculate the upper bound interval for F_1
  4: iter \leftarrow 1
                             5: \varepsilon_{1(iter)} \leftarrow {F_1}^*
                                    \triangleleft Set the first upper bound on F_1
  6: PF \leftarrow PF \cup [\mathbf{F}_1^*; \mathbf{F}_2(\mathbf{F}_1^*)]
                                                     \triangleleft Append the {F_1}^* corner point
  7: while iter \leq (PF^{size} - 2) do
         iter \leftarrow iter + 1

    □ Update the iteration counter

  9:
         \varepsilon_{1(iter)} \leftarrow \varepsilon_{1(iter-1)} + \varepsilon
                                                        \triangleleft Update the upper bound on F_1
         [F_1(F_{2(iter)}^*); F_{2(iter)}^*] \leftarrow SSP\text{-}CATL\text{-}2(InputData, \varepsilon_{1(iter)})
          PF \leftarrow PF \cup [\mathbf{F}_1(\mathbf{F}_{2(iter)}^*); \mathbf{F}_{2(iter)}^*]
                                                                        12: end while
                                                        \triangleleft Append the {F_2}^* corner point
13: PF \leftarrow PF \cup [F_1(F_2^*); F_2^*]
14: return PF
```

After obtaining the initial PF using the ECON method, ECON-GP estimates the objective intervals amongst the consecutive PF points (steps 1-5 in Algorithm 1) and checks if there are any PF segments that do not have the desired density (steps 6-22 in Algorithm 1). Since the objective  $F_2$  is minimized in the considered example, the objective intervals for  $F_2$  will be estimated. If the objective intervals do not satisfy a pre-determined requirement (defined using the GP tolerance value -GPtol), ECON-GP deploys the canonical GP method (step 16 in Algorithm 1). In the considered example, the  $F_2$  interval amongst PF points "1" and

tively. The SSP-CATL-1 mathematical model, aiming to minimize the objective  $F_1$  while imposing a certain bound on the objective  $F_2$ , can be formulated using additional equations (5-13)-(5-15). The SSP-CATL-2 mathematical model, aiming to minimize the objective  $F_2$  while imposing a certain bound on the objective  $F_1$ , can be represented using additional equations (5-16)-(5-18). For a more detailed description of the traditional ECON and GP methods, the interested readers can refer to

#### Mavrotas (2009) and Deb (1999).

GP: Goal Programming Method	
$min\left[\delta^{F_1}\cdot(\Delta F_1^+ + \Delta F_1^-) + \delta^{F_2}\cdot(\Delta F_2^+ + \Delta F_2^-) ight]$	(5-8)
Subject to: Constraints (4-3)-(4-7), (4-10)-(4-11)	, (4-13)-(4-30), and (5-3)-(5-7)
$F_1 = [\Lambda^{own} + \Lambda^{char} + \Lambda^{inv} + \Lambda^{late}]$	(5-9)
$F_2 = [A^{fuel} + A^{port} + A^{emis}]$	(5-10)
$m{F_1} - \Delta m{F}_1^+ + \Delta m{F}_1^- \ = m{F}_1^{target}$	(5-11)
$m{F}_2 - \Delta m{F}_2^+ + \Delta m{F}_2^- = m{F}_2^{target}$	(5-12)
<b>SSP-CATL-1:</b> SSP-CATL with $F_1$ Minimization	
$min F_1 = [\Lambda^{own} + \Lambda^{char} + \Lambda^{inv} + \Lambda^{late}]$	(5-13)
Subject to:	
Constraints (4-3)-(4-7), (4-10)-(4-11), (4-13)-(4-3	30), and (5-3)-(5-7)
$F_2 = [A^{fuel} + A^{port} + A^{emis}]$	(5-14)
$F_2 \leq arepsilon_2$	(5-15)
<b>SSP-CATL-2:</b> SSP-CATL with $F_2$ Minimization	
$min F_2 = [\Lambda^{fuel} + \Lambda^{port} + \Lambda^{emis}]$	(5-16)
Subject to:	

#### 6. Computational experiments and managerial insights

Constraints (4-3)-(4-7), (4-10)-(4-11), (4-13)-(4-30), and (5-3)-(5-7)

#### 6.1. Input data selection

 $F_1 = [\Lambda^{own} + \Lambda^{char} + \Lambda^{inv} + \Lambda^{late}]$ 

 $F_1 \leq \varepsilon_1$ 

The computational experiments were performed for the Europe Pakistan India Consortium 2 (EPIC-2) shipping route, which is currently serviced by the Compagnie Maritime d'Affrètement and Compagnie Générale Maritime (a.k.a., "CMA CGM") shipping line. A graphical illustration of the considered shipping route is provided in Fig. 5, where the length of voyage legs connecting consecutive ports is presented in square brackets. The adopted values of the input data that were used for the developed mixed integer multi-objective SSP-CATL mathematical model throughout the computational experiments are presented in Table 2. The input data were primarily adopted from the open data sources as well as the previous studies on liner shipping (Abioye et al., 2019; Ozcan et al., 2020; Zhao et al., 2020; CMA CGM, 2021; Pasha et al., 2021; Ports.com, 2021; Yu et al., 2021). The following sections of the manuscript focus on the evaluation of the proposed solution methodology and showcase certain important managerial insights using the developed multi-objective SSP-CATL mathematical model. A total of 20 problem instances were generated by altering the start and end of each

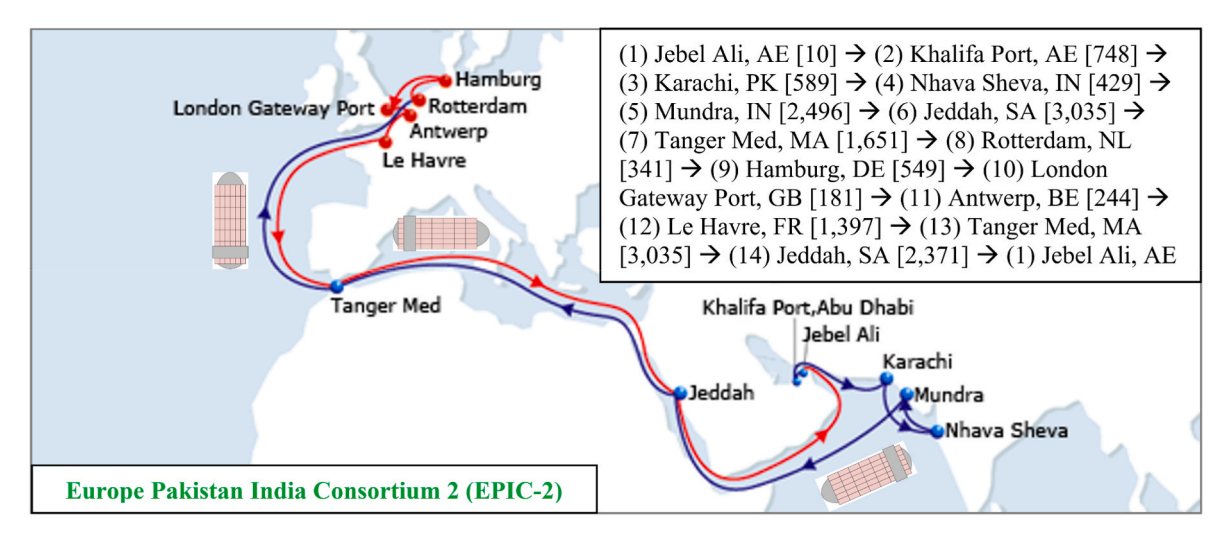
time window at ports of the considered shipping route to conduct the computational experiments.

#### 6.2. Evaluation of the proposed solution algorithm

# 6.2.1. ECON-GP sensitivity to the desired PF size and the ship sailing speed discretization level

The computational performance of the traditional ECON method is substantially affected with the desired PF size. Increasing PF size will increase the number of ECON iterations and, hence, will cause a CPU time increase. Since the ECON-GP method proposed in this study is based on the traditional ECON method, its computational performance will be affected with the desired PF size as well. Furthermore, since the original SSP-CAT model was linearized by means of ship sailing speed discretization (see section 5.1), the ECON-GP computational performance will be influenced with the adopted discretization level (i.e., higher discretization level will improve the ship fuel consumption accuracy but will cause a CPU time increase). As a part of the performed experiments, a supplemental analysis was conducted to assess the ECON-GP sensitivity to the desired PF size and the ship sailing speed discretization level. A CPU with Dell Intel(R) Core™ i7 Processor and 32 GB of RAM was utilized to execute ECON-GP for all the developed problem instances. The General Algebraic Modeling System (GAMS) was used to encode the GP, SSP-CATL-1, and SSP-CATL-2 mathematical models, which are directly deployed by ECON-GP (see section 5.2). CPLEX with a 0.01% optimality gap was deployed to solve the GP, SSP-CATL-1, and SSP-CATL-2 mathematical models within ECON-GP. The value of GPtol parameter was set to 1.5 based on the preliminary computational experiments, while the target objective violation penalties were set to  $\delta^{F_1} = \delta^{F_2} = 1.2$  USD/USD.

A total of 110 scenarios were evaluated throughout the analysis by changing the desired PF size from 10 points to 20 points with an increment of 1 point and by changing the discretization level from 5 points to 50 points with an increment of 5 points. The average CPU times incurred by ECON-GP for the generated scenarios over the developed problem instances are reported in Table 3. As expected, the CPU time generally increased with increasing values of the desired PF size and the ship sailing speed discretization level. However, the CPU time increases were more substantial after increasing the desired PF size when comparing to increases in the discretization level. In particular, the CPU time on average increased from 12.35 s to 13.75 s after increasing the discretization level from 5 points to 50 points. On the other hand, the CPU time on average increased from 8.09 s to 18.20 s after increasing the desired PF size from 10 points to 20 points. Nevertheless, the maximum CPU time did not exceed 20 s over all the generated scenarios,



(5-17)

(5-18)

Fig. 5. An illustration of the considered shipping route.

**Table 2**Input data for the developed multi-objective optimization model.

Model Parameter	Adopted Value
Total number of ports under a given port rotation – <i>a</i> (ports)	14
Total number of marine terminals available at port $p-b_p, p\in P$ (ports)	3
Total number of ship arrival time windows available at terminal $m$ of port $p-c_{pm}, p\in P, m\in M_p$ (time windows)	3
Total number of handling rates available at terminal $m$ of port $p$ during time window $t-d_{pmt}, p\in P, m\in M_p, t\in T_{pm}$ (rates)	4
Coefficients for ship fuel consumption – $\alpha, \gamma$	$\alpha=3,\gamma=0.012$
Average cargo weight inside a standard 20-ft container – $\varpi$ (tons)	11
Empty weight of a ship to be deployed – $\psi^{empty}$ (tons)	50,000
Total capacity of a ship to be deployed – $\psi^{cap}$ (tons)	150,000
Emission factor at sea – $\eta^{sea}$ (tons of emissions/ton of fuel)	3.114 <sup>a</sup>
Emission factor for the ship service under handling rate $h$ at terminal $m$ of port $p$ during time window $t - \eta_{pmth}^{oort}, p \in P, m \in M_p, t \in T_{pm}, h \in H_{pmt}$ (tons of emissions/TEU)	$0.01729 \text{ for } h = 180^{\text{ a}}$
Handling productivity for handling rate $h$ that will be used for the ship service at terminal $m$ of port $p$ during time window $t - \pi_{pmth}, p \in P, m \in M_p, t \in T_{pm}, h \in H_{pmt}$ (TEUs/hour)	<i>U</i> [50; 180]
Weekly operational cost of own ships – $\delta^{own}$ (USD/week)	200,000
Weekly cost of ship chartering – $\delta^{char}$ (USD/week)	300,000
Unit cost of container inventory – $\delta^{inv}$ (USD per TEU per hour)	0.5
Unit cost of ship late arrival at port $p - \delta_p^{late}$ (USD/hour)	U[5,000;10,000]
Unit cost of ship fuel at voyage leg $p - \delta_p^{fuel}$ (USD/ton)	[200; 500] <sup>b</sup>
Unit cost of ship service under handling rate $h$ at terminal $m$ of port $p$ during time window $t-\delta_{pmth}^{hand}, p\in P, m\in M_p, t\in T_{pm},$ $h\in H_{pmt}$ (USD/TEU)	<i>U</i> [300; 800]
Unit cost of ship emissions – $\delta^{emis}$ (USD/ton)	32 <sup>a</sup>
Total number of containers that will be carried at voyage $\log p - \varphi_p^{sea}, p \in P$ (TEUs)	U[5,000;10,000]
Total number of containers that will be handled at port $p-\varphi_p^{\text{port}}, p \in P$ (TEUs)	U[200;1,000]
Lower bound on ship sailing speed – $s^{min}$ (knots)	15
Upper bound on ship sailing speed – $s^{max}$ (knots)	25
Available number of own ships for deployment – $q^{own-max}$ (ships)	5
Available number of chartered ships for deployment – $q^{own-char}$ (ships)	8
Time window duration at port $p-[ au_{pmt}^{end}- au_{pmt}^{st}], p\in P, m\in M_p,$ $t\in T_{pm}$ (hours)	<i>U</i> [12; 24] <sup>c</sup>

#### Notes.

- $^{\rm a}$  The computational experiments were conducted considering carbon dioxide (CO<sub>2</sub>) as the main pollutant. However, without loss of generality, other pollutants can be evaluated using the proposed model as well.
- <sup>b</sup> Marine gas oil with low sulfur content and the unit cost of 500 USD/ton was used within the English channel, which is designated as the Emission Control Area. Alternative fuel oil with the unit cost of 200 USD/ton was used for the rest of voyage legs.
- c The end time for time window t at terminal m of port p (hours) was generated as follows:  $\tau_{(p+1)mt}^{end} = \tau_{pmt}^{end} + \frac{\lambda_p}{U[s^{min}; s^{max}]} \ \forall p \in P, m \in M_p, t \in T_{pm}.$

which can be viewed as acceptable. Therefore, the discretization level will be set to 50 points, while the desired PF size will be set to 20 points for the ECON-GP method throughout the computational experiments.

# ${\it 6.2.2.} \ \, {\it Evaluation of ECON-GP against the traditional ECON method}$

As a part of the performed experiments, a supplemental analysis was conducted to assess potential advantages of the developed ECON-GP method over the traditional ECON method. The latter task was accomplished by executing the traditional ECON method for all the developed 20 problem instances (i.e., the same instances that were solved by ECON-GP). The results from the performed analysis are summarized in Fig. 6 and Fig. 7. It can be observed that ECON-GP had to generate a total

of 7–8 PF points in addition to the desired PF size of 20 PF points for each of the problem instances developed (see Fig. 6). Additional PF points were required to meet the acceptable level of PF density. Indeed, the PF density obtained by the traditional ECON method was not sufficient for the considered problem instances, as significant  $F_2$  objective intervals were observed for some of the consecutive PF points (see Fig. 7). Large objective intervals are not desirable from the practical point of view, as they impose limitations in the analysis of trade-offs amongst the conflicting objectives. On the other hand, the issue of insufficient PF density has been effectively addressed by ECON-GP (see Fig. 7). Note that Fig. 7 shows the PFs obtained by ECON and ECON-GP for the problem instances "1"-"4". However, the same patterns were observed for the remaining problem instances as well.

# 6.3. Evaluation of the proposed mathematical model

#### 6.3.1. Analysis of the trade-offs amongst the conflicting objectives

As a part of the performed experiments, a supplemental analysis was conducted to evaluate the trade-offs amongst the conflicting objectives in the ship schedule design. The latter task was accomplished by extracting the solution data for the corner PF points obtained by ECON-GP for each one of the considered problem instances. Note that the corner PF points correspond to the points that have the best (i.e., the minimum) values of the objective functions  $F_1$  and  $F_2$  and are denoted in this manuscript as  $F_1^*$  and  $F_2^*$ , respectively (see Fig. 8, where the PF corner points and the entire PF are shown for the problem instance "1"). The results from the performed analysis are summarized in Table 4, where the following data are presented for every corner PF point and every problem instance: (i) the  $F_1$  objective value; (ii) the  $F_2$  objective value; (iii) the average ship sailing speed weighted by voyage leg length  $(s^w)$ ; (iv) the total ship waiting time at ports  $(\tau^{wait})$ ; (v) the total ship handling time at ports ( $\tau^{hand}$ ); (vi) the total ship sailing time at sea ( $\tau^{sail}$ ); (vii) the total late arrivals of ships at ports ( $\tau^{late}$ ); (viii) the total ship fuel consumption  $(\varphi)$ ; (ix) the total quantity of emissions released at sea  $(\xi^{sea})$ ; (x) the total quantity of emissions released at ports  $(\xi^{port})$ ; (xi) the total number of ships deployed (q); (xii) the total number of own ships deployed  $(q^{own})$ ; and (xiii) the total number of chartered ships deployed  $(q^{char}).$ 

Based on the outcomes from the performed analysis, it can be observed that the ship schedules with the  $F_1$  minimum values (i.e., the  $F_1^*$  ship schedules) are significantly different from the ship schedules with the  $F_2$  minimum values (i.e., the  $F_2^*$  ship schedules). In particular, if the shipping line decides to follow the environmental sustainability goals and select the  $F_2^*$  ship schedules, it will have to reduce the ship sailing speed by 25.32% when comparing to the  $F_1^*$  ship schedules. A decrease in the ship sailing speed may reduce the fuel consumption and the associated emissions produced by ships at sea by more than 45% for the  $F_2^*$  ship schedules. Furthermore, if the shipping line decides to follow the environmental sustainability goals and select the  $F_2^*$  ship schedules, the emissions produced by the designated handling equipment throughout the service of arriving ships at ports could be reduced by 59.74% when comparing to the  $F_1^*$  ship schedules by means of selecting lower handling rates. However, decreasing sailing speed of ships and handing rates at ports could increase the amount of time spent at sea and ports by 20.22% and 24.51%, respectively. An increase in the amount of time spent at sea and ports would further lead to an increase in the total turnaround time of ships. The conducted experiments show that the shipping line had to deploy an additional ship in each one of the considered problem instances to ensure the weekly port service frequency (i.e., a total of 6 ships were required for the  $F_2^*$  ship schedules, whereas 5 ships were sufficient for the  $F_1^*$  ship schedules). Moreover, larger late arrivals (but lower waiting times) were observed at ports for the  $F_2^*$  ship schedules as well.

In general, the  ${F_2}^*$  ship schedules allowed reducing the  $F_2$  objective

**Table 3**The average CPU time recorded for the generated scenarios (seconds).

$ K  \backslash PF^{size}$	10	11	12	13	14	15	16	17	18	19	20
5	7.45	7.79	9.80	9.89	11.90	11.77	13.10	14.27	15.78	15.92	18.16
10	7.41	8.54	9.73	10.37	11.81	11.83	13.84	13.56	14.37	15.76	17.03
15	7.78	8.13	9.79	10.01	11.81	12.05	13.51	14.20	15.24	16.86	17.88
20	8.21	9.03	10.54	11.15	12.31	12.43	13.84	14.36	16.35	17.04	17.94
25	8.29	9.05	10.72	10.40	12.78	12.74	14.52	14.64	16.39	16.90	17.20
30	8.19	9.31	10.46	10.40	12.98	13.77	14.49	15.39	16.63	17.53	18.79
35	7.94	8.56	10.49	11.51	12.80	13.18	14.91	15.91	15.98	17.83	18.13
40	8.33	9.37	11.03	11.46	12.57	12.74	15.21	15.48	17.82	17.72	18.78
45	8.98	9.67	11.25	12.84	13.54	13.41	14.74	16.27	16.58	17.81	18.69
50	8.31	9.85	11.20	12.13	13.56	13.56	14.18	15.66	16.18	17.28	19.40

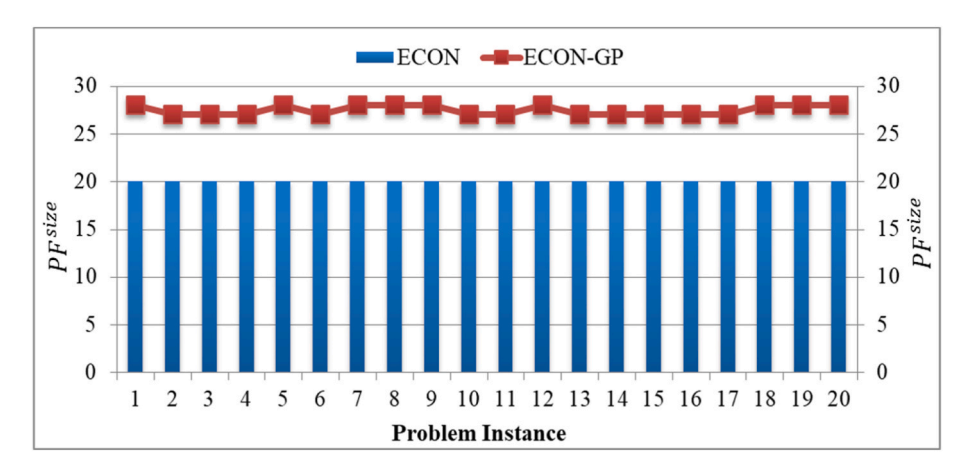


Fig. 6. The PF size of the ECON and ECON-GP methods for the considered problem instances.

by 36.18% when comparing to the  $F_1^*$  ship schedules but increased the  $F_1$  objective by 23.25%. Note that the corner PF points can be viewed as rather radical ship scheduling decisions (i.e., strictly follow the economic perspectives by selecting the  $F_1^*$  ship schedules or strictly follow the environmental perspectives by selecting the  $F_2^*$  ship schedules). However, there are many intermediate PF points identified by ECON-GP that compromise the conflicting objectives. For instance, the PF point "10" not only allows reducing the  $F_1$  value by 21.87%, when comparing to the  $F_1(F_2^*)$  point, but also decreases the  $F_2$  value by 19.08%, when comparing to the  $F_2(F_1^*)$  point (see Fig. 8). On the other hand, the PF point "18" not only allows reducing the  $F_1$  value by 12.15%, when comparing to the  $F_1({F_2}^*)$  point, but also decreases the  $F_2$  value by 22.24%, when comparing to the  $F_2(F_1^*)$  point (see Fig. 8). Therefore, the developed multi-objective SSP-CATL mathematical model and the proposed ECON-GP solution method can serve as an effective decision support system for shipping lines and assist with the analysis of tradeoffs amongst the conflicting objectives in the ship schedule design. More importantly, the proposed solution methodology will assist shipping lines with the identification of ship schedules that will compromise the economic and environmental perspectives.

# 6.3.2. Analysis of potential effects of collaborative agreements As a part of the performed experiments, a supplemental analysis was

conducted to evaluate potential effects of collaborative agreements amongst the shipping line and marine terminal operators on the ship schedule design (i.e., the availability of multiple marine terminals for service of the arriving ships along with the availability of multiple arrival time windows and handlings rates at those terminals). The latter task was accomplished by analyzing the following scenarios of collaborative agreements: (i) "3MTs-3TWs-4HRs" – the default collaborative agreements where 3 marine terminals are available at every port of the shipping route, and every terminal operator can offer 3 arrival time windows and 4 handling rates for service of ships; (ii) "1MT-3TWs-4HRs" - the alternative collaborative agreements where just 1 marine terminal is available at every port of the shipping route, and the terminal operator can offer 3 arrival time windows and 4 handling rates for service of ships; (iii) "3MTs-1TW-4HRs" - the alternative collaborative agreements where 3 marine terminals are available at every port of the shipping route, and every terminal operator can offer just 1 arrival time window and 4 handling rates for service of ships; and (iv) "3MTs-3TWs-1HR" - the alternative collaborative agreements where 3 marine terminals are available at every port of the shipping route, and every terminal operator can offer 3 arrival time windows and just 1 handling rate for service of ships.

The developed ECON-GP method was executed for all the generated scenarios of collaborative agreements and each one of the considered problem instances. The results from the performed analysis are

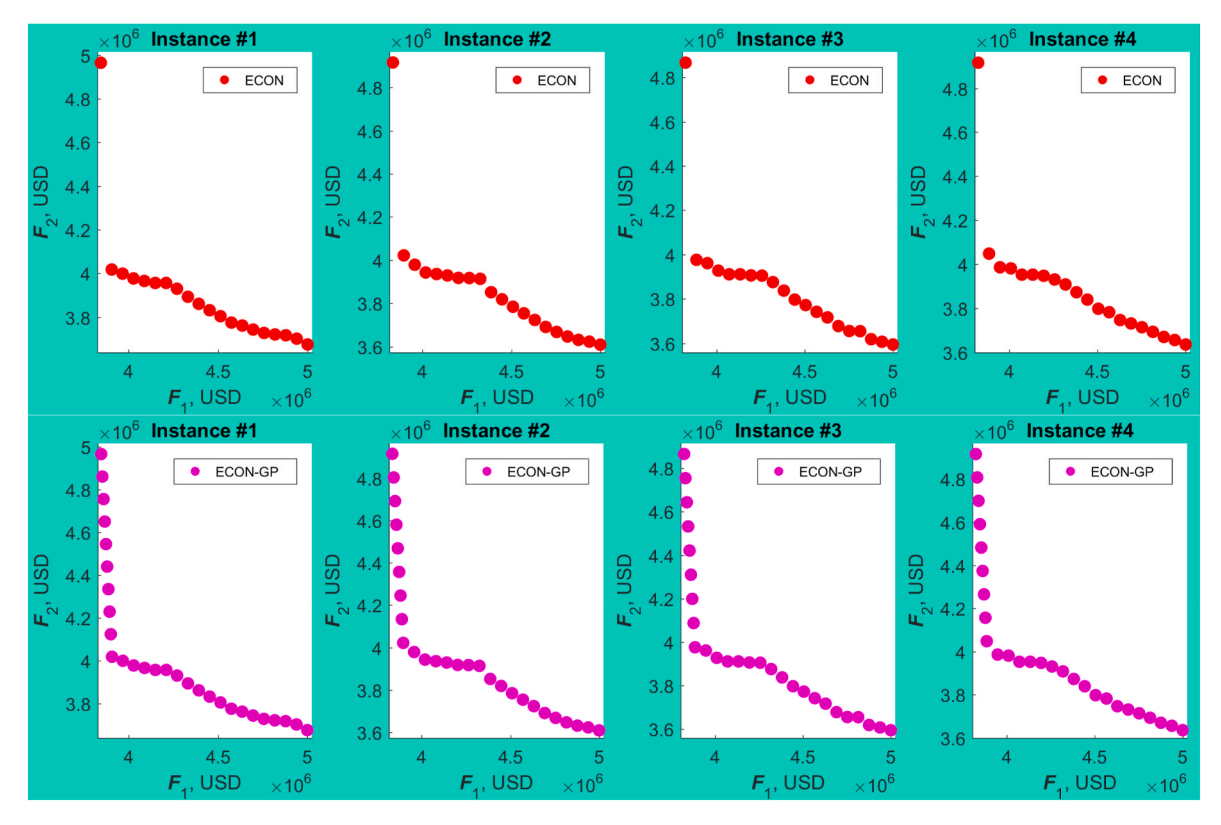


Fig. 7. The PFs obtained by the ECON and ECON-GP methods for the problem instances "1"-"4".

presented in Fig. 9 and Fig. 10. Based on the conducted analysis, superior PFs were observed for the first scenario of collaborative agreements (i.e., "3MTs-3TWs-4HRs") for each one of the considered problem instances. Such a finding highlights the importance of effective collaborative agreements amongst shipping lines and marine terminal operators on the ship schedule design as well as the importance of availability of multiple arrival time windows and handlings rates at those terminals for service of the arriving ships. Collaborative agreements amongst marine terminal operators and flexibility in terms of selection of arrival time windows and handlings rates allowed the shipping line designing more efficient ship schedules from both economic and environmental

perspectives. The quality of PFs started significantly declining after imposing certain restrictions in the existing collaborative agreements. The worst PFs were recorded for the scenario when only one handling rate was available at every terminal of every port for service of the arriving ships (i.e., scenario "3MTs-3TWs-1HR"). Therefore, effective collaborative agreements amongst shipping lines and marine terminal operators are essential for sustainable maritime transportation, as they can not only reduce the costs associated with the transportation process itself but also preserve the environment.

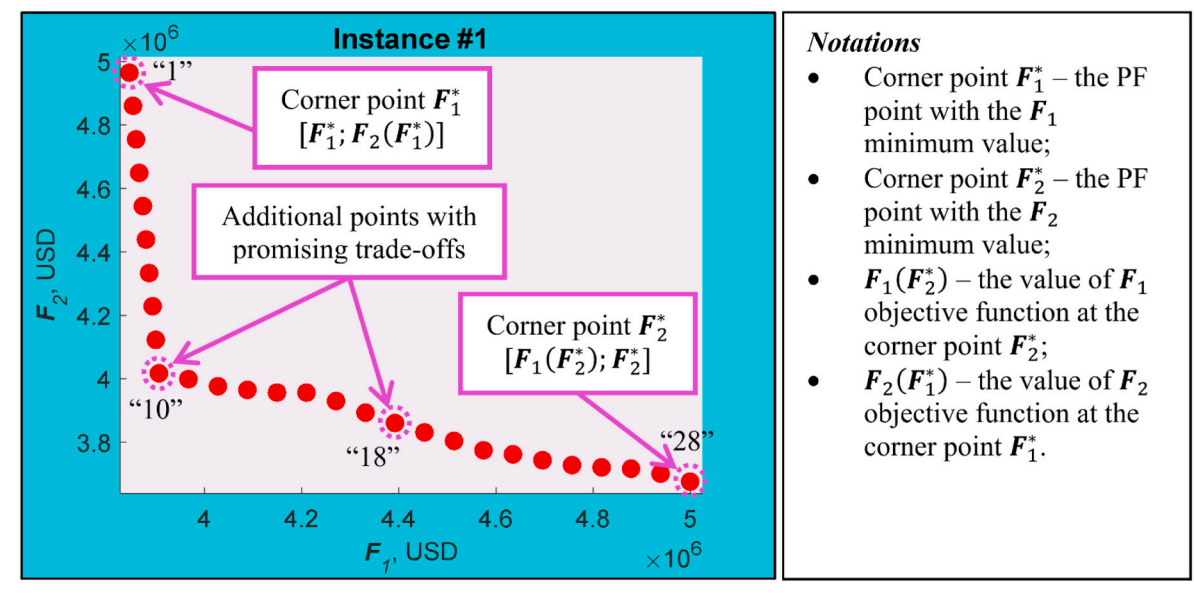


Fig. 8. Analysis of trade-offs amongst the conflicting objectives for the problem instance "1".

**Table 4**Solution data at the PF corner points for the considered problem instances.

Corner Poi	nt ${m F_1}^*$												
Instance	$F_1$ , 10 <sup>6</sup> USD	$F_2$ , $10^6$ USD	s <sup>w</sup> , knots	$ au^{wait}$ , hours	$ au^{hand}$ , hours	$ au^{sail}$ , hours	$ au^{late}$ , hours	$\varphi$ , tons	ξ <sup>sea</sup> , tons	ξ <sup>port</sup> , tons	q	$q^{own}$	qchar
1	3.846	4.965	25.00	55.53	101.43	683.04	2.81	4,158.00	12,814.96	73.08	5	4	1
2	3.835	4.916	25.00	51.09	105.87	683.04	1.48	4,158.00	12,814.96	69.00	5	4	1
3	3.825	4.866	25.00	47.36	109.60	683.04	0.00	4,158.00	12,814.96	64.65	5	4	1
4	3.825	4.917	25.00	60.36	96.60	683.04	0.00	4,158.00	12,814.96	71.95	5	4	1
5	3.825	4.894	25.00	50.54	106.42	683.04	0.00	4,158.00	12,814.96	70.01	5	4	1
6	3.841	4.847	25.00	48.98	107.98	683.04	2.20	4,158.00	12,814.96	70.33	5	4	1
7	3.861	4.926	25.00	56.23	100.73	683.04	3.72	4,158.00	12,814.96	76.34	5	4	1
8	3.846	4.966	25.00	62.24	94.72	683.04	2.48	4,158.00	12,814.96	74.35	5	4	1
9	3.825	4.974	25.00	52.15	104.81	683.04	0.00	4,158.00	12,814.96	70.14	5	4	1
10	3.839	4.908	25.00	54.71	102.25	683.04	1.52	4,158.00	12,814.96	73.00	5	4	1
11	3.839	4.981	25.00	53.95	103.01	683.04	2.68	4,158.00	12,814.96	73.91	5	4	1
12	3.825	4.984	25.00	57.84	99.12	683.04	0.00	4,158.00	12,814.96	77.33	5	4	1
13	3.859	4.989	25.00	55.16	101.80	683.04	3.65	4,158.00	12,814.96	74.80	5	4	1
14	3.848	4.980	25.00	52.31	104.65	683.04	3.32	4,158.00	12,814.96	73.43	5	4	1
15	3.825	4.952	25.00	57.98	98.98	683.04	0.00	4,158.00	12,814.96	75.80	5	4	1
16	3.830	4.902	25.00	57.55	99.41	683.04	0.61	4,158.00	12,814.96	73.31	5	4	1
17	3.829	4.956	25.00	51.35	105.61	683.04	0.64	4,158.00	12,814.96	75.70	5	4	1
18	3.861	4.926	25.00	56.23	100.73	683.04	3.72	4,158.00	12,814.96	76.34	5	4	1
19	3.846	4.966	25.00	62.24	94.72	683.04	2.48	4,158.00	12,814.96	74.35	5	4	1
20	3.825	4.974	25.00	52.15	104.81	683.04	0.00	4,158.00	12,814.96	70.14	5	4	1
Average:	3.838	4.939	25.00	54.80	102.16	683.04	1.57	4,158.00	12,814.96	72.90	5	4	1
Corner Poi	nt ${F_2}^*$												
Instance	$F_1$ , 10 <sup>6</sup> USD	$F_2$ , $10^6$ USD	sw, knots	$ au^{wait}$ , hours	$ au^{hand}$ , hours	$ au^{sail}$ , hours	$ au^{late}$ , hours	$\varphi$ , tons	ξ <sup>sea</sup> , tons	ξ <sup>port</sup> , tons	q	$q^{own}$	<b>q</b> <sup>char</sup>
1	5.000	3.675	20.38	37.85	132.11	838.04	26.23	2,916.54	8,988.78	47.91	6	5	1
2	5.000	3.609	19.58	0.32	135.45	872.24	14.39	2,757.30	8,498.00	45.22	6	5	1
3	5.000	3.594	19.75	10.32	133.06	864.61	16.51	2,842.02	8,759.09	46.02	6	5	1
4	5.000	3.636	19.58	0.78	135.14	872.08	14.83	2,883.96	8,888.37	45.79	6	5	1
5	5.000	3.688	20.40	39.99	130.99	837.01	31.29	3,053.64	9,411.33	47.56	6	5	1
6	5.000	3.589	19.90	10.29	139.70	858.02	17.39	2,832.26	8,729.02	42.98	6	5	1
7	5.000	3.642	20.21	29.63	133.34	845.03	25.48	2,870.22	8,846.03	47.83	6	5	1
8	5.000	3.604	19.74	8.40	134.50	865.10	18.47	2,884.81	8,890.99	44.43	6	5	1
9	5.000	3.646	20.17	23.22	138.18	846.61	25.34	2,947.84	9,085.23	43.14	6	5	1
10	5.000	3.650	20.18	28.16	133.75	846.08	31.97	2,889.71	8,906.08	47.50	6	5	1
11	5.000	3.621	19.71	8.23	133.47	866.29	14.83	2,801.82	8,635.21	45.31	6	5	1
12	5.000	3.689	20.62	43.47	136.42	828.11	38.30	3,053.26	9,410.16	46.60	6	5	1
13	5.000	3.597	19.84	7.43	139.71	860.86	21.48	2,796.53	8,618.90	42.89	6	5	1
14	5.000	3.579	19.69	1.93	138.88	867.19	16.43	2,718.22	8,377.54	44.30	6	5	1
15	5.000	3.625	19.77	10.69	133.54	863.77	19.66	2,826.80	8,712.21	47.15	6	5	1
16	5.000	3.608	19.77	5.08	139.19	863.73	16.74	2,791.72	8,604.08	44.46	6	5	1
17	5.000	3.595	19.57	2.42	133.02	872.56	16.18	2,711.78	8,357.72	48.18	6	5	1
18	5.000	3.642	20.21	29.63	133.34	845.03	25.48	2,870.22	8,846.03	47.83	6	5	1
	5.000	3.604	19.74	8.40	134.50	865.10	18.47	2,884.81	8,890.99	44.43	6	5	1
19	3.000	0.001	17.71	0.10									
19 20	5.000	3.646	20.17	23.22	138.18	846.61	25.34	2,947.84	9,085.23	43.14	6	5	1

## 7. Conclusions

As the amount of emissions produced by oceangoing ships is still ranked as "high" by the International Maritime Organization (IMO) and other relevant agencies, shipping lines have to explore innovative and effective alternatives to ensure sustainable development of maritime transportation and meet the long-term IMO targets. One of the effective options to meet the long-term IMO targets and ensure sustainable development of liner shipping is collaborative agreements amongst shipping lines and other industry partners (e.g., marine terminal operators that are directly involved in service of the arriving ships at ports). The main advantage of introducing collaborative agreements compared to other alternatives for emission reduction consists in the fact that collaborative agreements do not require significant monetary investments and can be executed amongst the relevant stakeholders by simply utilizing the available resources in a more effective manner. Therefore, this study proposed a novel multi-objective mathematical model for sustainable ship scheduling in liner shipping that explicitly captured comprehensive collaborative agreements amongst shipping lines and marine terminal operators.

Based on the collaborative agreements proposed, the shipping line

was not only able to select the marine terminal for the ship service at every port of the shipping route but also requested the appropriate arrival time window and handling rate. The first objective of the model minimized the cost components that are mostly driven by the economic perspectives, while the second one directly captured the environmental perspectives as well. A novel customized exact multi-objective optimization method (ECON-GP), inspired by the  $\varepsilon$ -constraint method (ECON) and the goal programming method (GP), was developed to solve the problem. The computational experiments were performed for the Europe Pakistan India Consortium 2 (EPIC-2) shipping route. It was found that the developed ECON-GP method was more efficient than the traditional ECON method, as it was able to generate the Pareto Fronts with sufficient solution density within a reasonable amount of computational time. Furthermore, the conducted computational experiments showcased how the proposed multi-objective mathematical model and the developed ECON-GP solution method could be used for the analysis of trade-offs amongst the economic and environmental perspectives in the ship schedule design. Last but not least, the experiments underlined the importance of collaborative agreements amongst the shipping line and marine terminal operators. Effective collaborative agreements amongst shipping lines and marine terminal operators, as the ones

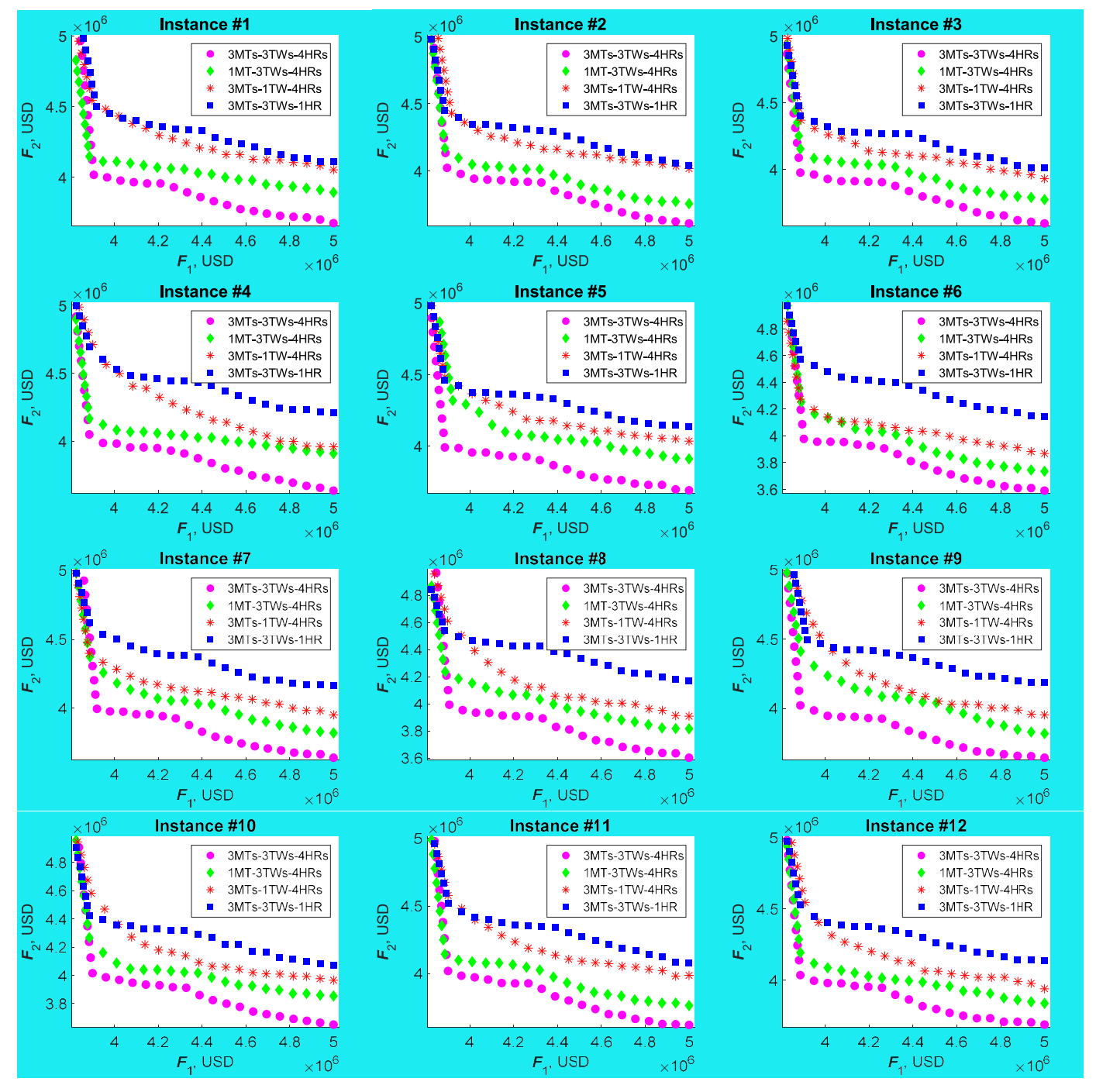


Fig. 9. The PFs obtained by the ECON-GP method for the generated scenarios of collaborative agreements and problem instances "1" through "12".

proposed in this study, are essential for sustainable maritime transportation, as they can not only reduce the costs associated with the transportation process itself but also preserve the environment.

A number of future research opportunities for this study can be explored. First, different methods for a robust ship schedule design, taking into account various uncertainties in the liner shipping operations, could be explicitly evaluated. Second, game-theoretic collaborative agreements amongst shipping lines and marine terminal operators could be investigated to capture the negotiation process of arrival time windows and handling rates at ports. Third, the container demand

variability due to various factors (e.g., transit time, geographic location, product type) could be modeled within the proposed multi-objective framework. Fourth, collaborative agreements amongst shipping lines (i.e., collaborations with the alliance partners) could be explored further using the developed multi-objective mathematical model. Fifth, additional historical data could be collected from ships to develop a more accurate fuel consumption model for the main ship engines. Moreover, other types of emissions released by oceangoing ships could be quantified using the presented multi-objective mathematical model.

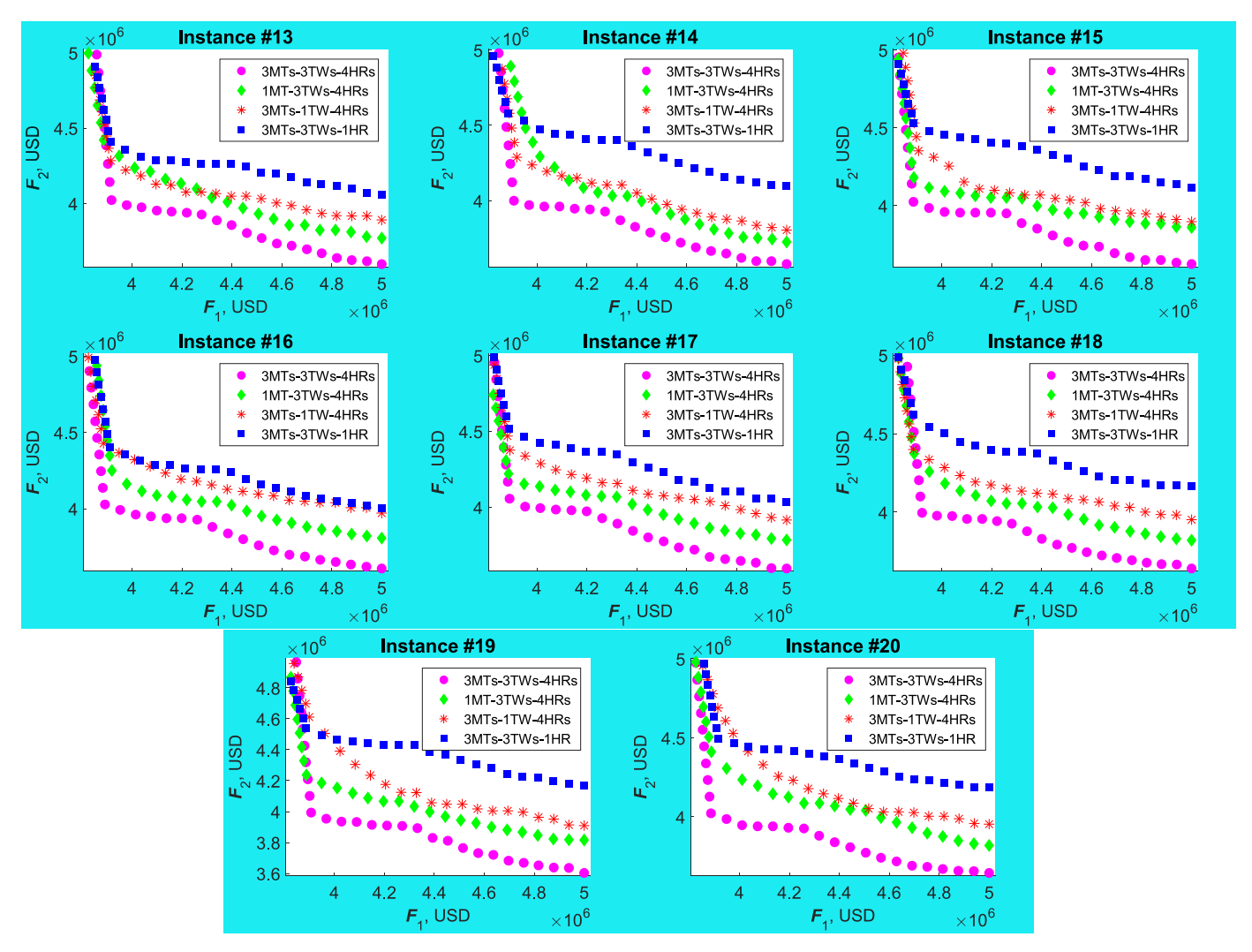


Fig. 10. The PFs obtained by the ECON-GP method for the generated scenarios of collaborative agreements and problem instances "13" through "20".

#### CRediT authorship contribution statement

**Maxim A. Dulebenets:** Conceptualization, Methodology, Data curation, Visualization, Investigation, Writing – original draft, Writing – review & editing.

# Declaration of competing interest

The authors declare that they have no known competing financial interests or personal relationships that could have appeared to influence the work reported in this paper.

# Acknowledgments

This work has been partially supported by the National Science Foundation grant CMMI-1901109. The opinions, findings, and conclusions, expressed in this publication, are those of the authors and do not necessarily reflect the views of the National Science Foundation.

# References

Abioye, O.F., Dulebenets, M.A., Pasha, J., Kavoosi, M., 2019. A vessel schedule recovery problem at the liner shipping route with emission control areas. Energies 12 (12), 2290.

Adland, R.O., Jia, H., 2016. Vessel speed analytics using satellite-based ship position data. In: Paper Presented at the 2016 IEEE International Conference on Industrial

Engineering and Engineering Management (IEEM). Retrieved on 04/23/2021 from. https://ieeexplore.ieee.org/document/7798088.

Alharbi, A., Wang, S., Davy, P., 2015. Schedule design for sustainable container supply chain networks with port time windows. Adv. Eng. Inf. 29 (3), 322–331.

Bierwirth, C., Meisel, F., 2015. A follow-up survey of berth allocation and quay crane scheduling problems in container terminals. Eur. J. Oper. Res. 244 (3), 675–689. Bouman, E., Lindstad, E., Rialland, A., Strømman, A., 2017. State-of-the-art technologies,

Bouman, E., Lindstad, E., Rialland, A., Strømman, A., 2017. State-of-the-art technologies measures, and potential for reducing GHG emissions from shipping – a review. Transport. Res. Transport Environ. 52 (A), 408–421.

Carlo, H.J., Vis, I.F., Roodbergen, K.J., 2015. Seaside operations in container terminals: literature overview, trends, and research directions. Flex. Serv. Manuf. J. 27 (2), 224–262.

Cho, S.W., Park, H.J., Lee, C., 2021. An integrated method for berth allocation and quay crane assignment to allow for reassignment of vessels to other terminals. Marit. Econ. Logist. 23 (1), 123–153.

CMA CGM, 2021. Europe Pakistan India Consortium 2. Retrieved on 04/10/2021 from. https://www.cma-cgm.com/products-services/line-services/flyer/EPIC2.

De, A., Mamanduru, V., Gunasekaran, A., Subramanian, N., Tiwari, M., 2016. Composite particle algorithm for sustainable integrated dynamic ship routing and scheduling optimization. Comput. Ind. Eng. 96, 201–215.

Deb, K., 1999. July. Solving goal programming problems using multi-objective genetic algorithms. In: Proceedings of the 1999 Congress on Evolutionary Computation-CEC99 (Cat. No. 99TH8406), vol. 1. IEEE, pp. 77–84.

Dong, G., Lee, P.T.W., 2020. Environmental effects of emission control areas and reduced speed zones on container ship operation. J. Clean. Prod. 274, 122582.

Dulebenets, M.A., 2016. Advantages and disadvantages from enforcing emission restrictions within emission control areas. Maritime Business Rev. 1 (2), 107–132.
 Dulebenets, M.A., 2018. A comprehensive multi-objective optimization model for the vessel scheduling problem in liner shipping. Int. J. Prod. Econ. 196, 293–318.

Dulebenets, M.A., 2019. Minimizing the total liner shipping route service costs via application of an efficient collaborative agreement. IEEE Trans. Intell. Transport. Syst. 20 (1), 123–136.

- Dulebenets, M.A., Golias, M.M., Mishra, S., 2018. A collaborative agreement for berth allocation under excessive demand. Eng. Appl. Artif. Intell. 69, 76–92.
- Dulebenets, M.A., Pasha, J., Abioye, O.F., Kavoosi, M., 2021. Vessel scheduling in liner shipping: a critical literature review and future research needs. Flex. Serv. Manuf. J. 33 (1), 43–106.
- Fagerholt, K., 2001. Ship scheduling with soft time windows: an optimization based approach. Eur. J. Oper. Res. 131, 559–571.
- Fathollahi-Fard, A.M., Hajiaghaei-Keshteli, M., Mirjalili, S., 2018. Multi-objective stochastic closed-loop supply chain network design with social considerations. Appl. Soft Comput. 71, 505–525.
- Fathollahi-Fard, A.M., Woodward, L., Akhrif, O., 2021. Sustainable distributed permutation flow-shop scheduling model based on a triple bottom line concept. J. Industrial Inform. Integration 100233.
- Gürel, S., Shadmand, A., 2019. A heterogeneous fleet liner ship scheduling problem with port time uncertainty. Cent. Eur. J. Oper. Res. 27 (4), 1153–1175.
- Imai, A., Nishimura, E., Papadimitriou, S., 2008. Berthing ships at a multi-user container terminal with a limited quay capacity. Transport. Res. E Logist. Transport. Rev. 44 (1), 136–151.
- IMO, 2020. Fourth IMO GHG study 2020 final report. Retrieved on 06/23/2021 from. https://www.imo.org.
- IMO, 2021a. IMO 2020 cutting sulphur oxide emissions. Retrieved on 06/25/2021 from. https://www.imo.org/en/MediaCentre/HotTopics/Pages/Sulphur-2020.aspx
- IMO, 2021b. Air pollution, energy efficiency and greenhouse gas emissions. Retrieved on 06/25/2021 from. https://www.imo.org.
- JOC, 2020. Houston container terminals to reopen after COVID-19 closures. Retrieved on 10/15/2021 from. https://www.joc.com.
- Kontovas, C., 2014. The Green Ship Routing and Scheduling Problem (GSRSP): A Conceptual Approach, vol. 31. Transportation Research Part D: Transport and Environment. pp. 61–69.
- Liu, Z., Wang, S., Du, Y., Wang, H., 2016. Supply chain cost minimization by collaboration between liner shipping companies and port operators. Transport. J. 55 (3), 296–314.
- Ma, W., Ma, D., Ma, Y., Zhang, J., Wang, D., 2021. Green maritime: a routing and speed multi-objective optimization strategy. J. Clean. Prod. 305, 127179.
- Mallidis, I., Iakovou, E., Dekker, R., Vlachos, D., 2018. The impact of slow steaming on the carriers' and shippers' costs: the case of a global logistics network. Transport. Res. E Logist, Transport, Rev. 111, 18–39.
- Mavrotas, G., 2009. Effective implementation of the  $\epsilon$ -constraint method in multiobjective mathematical programming problems. Appl. Math. Comput. 213 (2), 455–465.
- Meng, Q., Wang, S., Andersson, H., Thun, K., 2014. Containership routing and scheduling in liner shipping: overview and future research directions. Transport. Sci. 48 (2), 265–280.
- Ozcan, S., Eliiyi, D., Reinhardt, L., 2020. Cargo allocation and vessel scheduling on liner shipping with synchronization of transshipments. Appl. Math. Model. 77 (1),
- Pasha, J., Dulebenets, M.A., Fathollahi-Fard, A.M., Tian, G., Lau, Y.Y., Singh, P., Liang, B., 2021. An integrated optimization method for tactical-level planning in liner shipping with heterogeneous ship fleet and environmental considerations. Adv. Eng. Inf. 48, 101299.
- Pasha, J., Dulebenets, M.A., Kavoosi, M., Abioye, O.F., Theophilus, O., Wang, H., Kampmann, R., Guo, W., 2020. Holistic tactical-level planning in liner shipping: an exact optimization approach. J. Shipping Trade 5 (1), 1–35.
- Peng, J., Zhou, Z., Li, R., 2015. A collaborative berth allocation problem with multiple ports based on genetic algorithm. J. Coast Res. 73 (1), 290–297.

- Peng, Y., Dong, M., Li, X., Liu, H., Wang, W., 2021. Cooperative optimization of shore power allocation and berth allocation: a balance between cost and environmental benefit. J. Clean. Prod. 279, 123816.
- Ports.com, 2021. Sea route & distance. Retrieved on 04/23/2021 from. http://ports.com/sea-route/.
- Psaraftis, H.N., Kontovas, C.A., 2013. Speed models for energy-efficient maritime transportation: a taxonomy and survey. Transport. Res. C Emerg. Technol. 26, 221, 251
- Qi, J., Zheng, J., Yang, L., Yao, F., 2021. Impact analysis of different container arrival patterns on ship scheduling in liner shipping. Marit. Pol. Manag. 48 (3), 331–353.
- Ronen, D., 2011. The effect of oil price on containership speed and fleet size. J. Oper. Res. Soc. 62 (1), 211–216.
- Song, D.P., Li, D., Drake, P., 2015. Multi-objective optimization for planning liner shipping service with uncertain port times. Transport. Res. E Logist. Transport. Rev. 84, 1–22.
- Tang, W., Li, H., Chen, J., 2021. Optimizing carbon taxation target and level: enterprises, consumers, or both? J. Clean. Prod. 282, 124515.
- Torkian, F., Hoseini, S.F., Askarpoor, H., 2020. A berth allocation policy by considering collaboration between adjacent container terminals. J. Qual. Eng. Prod. Optimization 5 (2), 87–104.
- Tran, N.K., Haasis, H.D., Buer, T., 2017. Container shipping route design incorporating the costs of shipping, inland/feeder transport, inventory and CO2 emission. Marit. Econ. Logist. 19 (4), 667–694.
- UNCTAD, 2020. Review of maritime transport 2020. Retrieved on 04/23/2021 from. https://unctad.org/en/PublicationsLibrary/rmt2020\_en.pdf.
- Wang, S., Meng, Q., 2012. Sailing speed optimization for container ships in a liner shipping network. Transport. Res. E Logist. Transport. Rev. 48 (3), 701–714.
- Wang, S., Meng, Q., 2017. Container liner fleet deployment: a systematic overview. Transport. Res. C Emerg. Technol. 77, 389–404.
- Wang, S., Alharbi, A., Davy, P., 2014. Liner ship route schedule design with port time windows. Transport. Res. C Emerg. Technol. 41, 1–17.
- Wang, S., Liu, Z., Qu, X., 2015. Collaborative mechanisms for berth allocation. Adv. Eng. Inf. 29 (3), 332–338.
- Wang, S., Meng, Q., Liu, Z., 2013. Bunker consumption optimization methods in shipping: a critical review and extensions. Transport. Res. E Logist. Transport. Rev. 53, 49–62.
- Wang, Y., Wang, S., 2021. Deploying, scheduling, and sequencing heterogeneous vessels in a liner container shipping route. Transport. Res. E Logist. Transport. Rev. 151, 102365
- Wang, Y., Meng, Q., Kuang, H., 2019. Intercontinental liner shipping service design. Transport. Sci. 53 (2), 344–364.
- Wen, M., Pacino, D., Kontovas, C., Psaraftis, H., 2017. A Multiple Ship Routing and Speed Optimization Problem under Time, Cost and Environmental Objectives, vol. 52. Transportation Research Part D: Transport and Environment, pp. 303–321.
- Yang, L., Cai, Y., Wei, Y., Huang, S., 2019. Choice of technology for emission control in port areas: a supply chain perspective. J. Clean. Prod. 240, 118105.
- Yu, Y., Tu, J., Shi, K., Liu, M., Chen, J., 2021. Flexible optimization of international shipping routes considering carbon emission cost. Math. Probl Eng. 2021, 6678473.
- Zhao, Y., Zhou, J., Fan, Y., Kuang, H., 2020. Sailing speed optimization model for slow steaming considering loss aversion mechanism. J. Adv. Transport, 2020, 2157945.
- Zhuge, D., Wang, S., Wang, D.Z., 2021. A joint liner ship path, speed and deployment problem under emission reduction measures. Transp. Res. Part B Methodol. 144, 155–173